

**CARDIOVASCULAR ACTIVITIES OF
LORANTHUS FERRUGINEUS ROXB. METHANOL
EXTRACT AND ITS FRACTIONS**

OMAR ZIAD AMEER

UNIVERSITI SAINS MALAYSIA

2009

**AKTIVITI KARDIOVASKULAR EKSTRAK METANOL
LORANTHUS FERRUGINEUS ROXB. DAN FRAKSINYA**

oleh

OMAR ZIAD AMEER

**Tesis yang diserahkan untuk
memenuhi keperluan bagi
ijazah Sarjana Sains**

UNIVERSITI SAINS MALAYSIA

Mei 2009

**CARDIOVASCULAR ACTIVITIES OF *LORANTHUS FERRUGINEUS* ROXB.
METHANOL EXTRACT AND ITS FRACTIONS**

by

OMAR ZIAD AMEER

**Thesis submitted in fulfillment of the requirements
for the degree of
Master of Science**

UNIVERSITI SAINS MALAYSIA

May 2009

*This thesis is dedicated to
my beloved parents and brother*

ACKNOWLEDGEMENTS

In most of mankind, gratitude is merely a secret hope for greater favors

- *Duc de la Rochefoucauld, Maxims (1665)*

I sincerely acknowledge Allah's Knowledge and Wisdom in guiding, enriching and giving me sound mind every day to complete this study.

Studying for this M.Sc. degree was made possible by commitment from individuals, organizations and institutions. It is vital that I acknowledge their assistance, contribution and commitment.

This thesis owes its existence to the help, support, and inspiration of many people. In the first place, I would like to express my sincere appreciation and gratitude to my supervisor, Prof. Mohamad Zaini Asmawi, for his unlimited support and encouragement during the past two and a half years of my research. He has provided an optimum working environment at the Department of Pharmacology, School of Pharmaceutical Sciences, Universiti Sains Malaysia. His perpetual energy and enthusiasm in research had motivated all his advisees, including me. In addition, he was always accessible and willing to help his students with their research. As a result, research life became smooth and rewarding for me. His uncompromising quest for excellence significantly shapes everyone at the department.

I am also indebted to Asso. Prof. Amirin Sadikun, who has not only been a source of enthusiasm and encouragement, but has also agreed, with his exceptional insights into chemistry, to serve and enrich my knowledge in the phytochemistry part of my research.

I was delighted to interact with my co-advisor, Asso. Prof. Amin Malik Shah, who sets an example of a world-class researcher for his rigor and passion on research. Your generous invitations and wonderful trips did really enlighten the darkest hours I had during pursuing my research.

I offer a very special appreciation to Prof. Zhari Ismail, Department of Pharmaceutical Chemistry, School of Pharmaceutical Sciences, Universiti Sains Malaysia for the use of his department facilities.

I wish to extend my heartfelt gratitude to Prof. Munavvar Zubaid Abdul Sattar who, as well as allowing me to have access to his Physiology Department, cheerfully provided something much greater in all the years I have known him: a friendly smile and a hello every time we met.

I gratefully acknowledge Dr. Mohammad Jamshed Ahmad Siddiqui, Department of Pharmaceutical Chemistry, School of Pharmaceutical Sciences, Universiti Sains Malaysia for his advice and crucial contribution, which made him a backbone of this research and so to this thesis. His involvement with his originality and high professionalism in chemistry has triggered and nourished my intellectual maturity that I will benefit from, for a long time to come.

I have also benefited by advice and guidance from Dr. Hassan Hadi Abd Allah who was always generous with his time, kindly answering even my unintelligent questions about my research topic. Many thanks, brother, for your guidance.

All my lab buddies at the Pharmacology Department made it a convivial place to work. In particular, I would like to thank Mr. Raghava Naidu Sriramaneni, Mr. Mun Fei Yam, Mr. Ali Jimale, Mr. Subramaniam Rammohan, Mr. Mahfoudh Al-Mosali, Mr. Khaled Al-Gariri and Ms. Vanessa Daniel.

In my daily work I have also been blessed with a friendly and cheerful group of fellow students. In particular, I am pleased to acknowledge Ms. Hafsa Suhail Najim, Mr. Hayder Bahaa Sahib, Mr. Kolla R.L. Anand Swarup, Ms. Fatihah binti Basri, Ms. NurJannah binti Mohamad Hussian and Ms. Zunoliza binti Abdullah. Many thanks to you guys for your friendship and indispensable help in the past few years.

Collective and individual acknowledgments are also owed to all the technical and non-technical staff of the School of Pharmaceutical Sciences, Universiti Sains Malaysia. Many thanks go in particular to Mr. Yosuff Md. Saud and Mr. Adnan Omar from the Animal House Facility, Mr. Roseli Hassan, Mr. Adnan Jaafar, Mr. Mohamad Hassan Haji Ramli, Mr. Abd. Rahim Abdullah, Mr. Abd. Malek Mustaffa, Mr. Santhus Stanley Francis, Mr. Selvamani a/l Narayanan Nair, Mr. Basri Jaafar, Ms. Yong Mee Nyok, the former deputy dean Dr. Pazilah Ibrahim, the present deputy dean Dr. Mohamed Izham Mohamed Ibrahim, the former dean Dr. Abbas Hj. Hussin and the present deputy dean Dr. Syed Azhar Syed Sulaiman.

I have greatly appreciated the generous financial support from the Institute of Graduate Studies, Universiti Sains Malaysia through Universiti Sains Malaysia fellowship award. In reflection, I am overcome by the confidence of the trustees who granted me the fellowship, though, I am sure, my application was not one of the most outstanding ones. Without their support, my ambition to study abroad could have hardly been realized.

Words fail me to express my heartfelt appreciation to my best friend, Mr. Ibrahim M. Salman. Without your help, Ibrahim, I would not have done much in this research. You will always be in my heart as a sincere brother and lovely person.

My deepest gratitude goes to my family for their unflagging love and support throughout my life; this dissertation is simply impossible without them. I am indebted to my father, Mr. Ziad Ameer, for his care and love. As a typical father in an Iraqi family, he worked industriously to support the family and spare no effort to provide the best possible environment for me to grow up and attend school. He had never complained in spite of all the hardships in his life. Although he is no longer with us, he is forever remembered. I am sure he shares our joy and happiness in the heaven. I cannot ask for more from my mother, Mrs. Rabihah Jasim, as she is simply perfect. I have no suitable word that can fully describe her everlasting love to me. I remember her constant support when I encountered difficulties and I remember, most of all, her delicious dishes. Mother, I love you. I feel proud of my brother, Mr. Ali Ziad, for his multitalents. He had been a raw model for me to follow unconsciously when I was a teenager and has always been one of my best counselors.

Finally, I would like to thank anyone else I may have failed to mention who contributed to the successful realization of this thesis. Obviously I have failed to mention the poor rats and guinea pigs who were made to give so much sacrifice for the sake of knowledge. May they rest in eternal peace and may God have mercy on my soul for what I did!



Omar Ziad Ameer
May 2009

TABLE OF CONTENTS

	Page
Acknowledgements	ii
Table of Contents	iv
List of Tables	x
List of Figures	xi
List of Abbreviations	xvii
Abstrak	xxi
Abstract	xxiii
CHAPTER 1 - INTRODUCTION	1
1.1 The circulatory system	1
1.1.1 The systemic and pulmonary circulation	1
1.1.2 The heart	4
1.1.2.1 Anatomy	4
1.1.2.2 Cardiac muscle	5
1.1.2.3 Cardiac innervation	6
1.1.2.4 Cardiac blood supply	6
1.1.2.5 Physiology of cardiac muscle contraction	6
1.1.2.5.a Action potential	7
1.1.2.5.b Cardiac contraction	8
1.1.3 Arteries and arterioles	9
1.1.3.1 Arterial blood pressure	10
1.1.3.2 Flow, pressure and resistance	11
1.1.4 Regulation of blood pressure	12
1.1.4.1 Sympathetic nervous system (SNS)	12
1.1.4.2 Renin-angiotensin-aldosterone system (RAAS)	12
1.1.4.3 Mosaic theory	13
1.1.4.4 Fluid volume regulation	13
1.1.5 Endothelial cells	13
1.1.5.1 Endothelial vasodilating factors	14
1.1.5.1.a Endothelium-derived relaxation factor (EDRF)	14
1.1.5.1.a.i Vasodilator effects of NO	16

1.1.5.1.a.ii	Modulation of sympathetic activity	18
1.1.5.1.a.iii	Antiplatelet effects of NO	19
1.1.5.1.a.iv	Antiadhesive effects of NO	20
1.1.5.1.a.v	Antiproliferative effects of NO	21
1.1.5.1.a.vi	Antioxidant effects of NO	21
1.1.5.1.b	Prostacyclins (PGI ₂)	24
1.1.5.1.c	Endothelium-derived hyperpolarizing factor (EDHF)	25
1.1.5.2	Endothelial vasoconstricting factors	27
1.1.5.2.a	Endothelins (ETs)	27
1.1.5.2.b	Angiotensin II (Ang II)	29
1.1.5.2.c	Arachidonic acid derivatives	29
1.1.5.2.c.i	Isoprostanes	29
1.1.5.2.c.ii	Thromboxane A ₂ (TXA ₂)	30
1.1.5.2.c.iii	Prostaglandin H ₂ (PGH ₂)	30
1.1.6	Vascular smooth muscle	31
1.1.6.1	Vascular smooth muscle contraction	31
1.1.6.2	Vascular smooth muscle relaxation	33
1.2	Ion channels	34
1.2.1	Calcium channels	34
1.2.2	Potassium channels	36
1.2.2.1	Delayed rectifier potassium channels (K _v)	37
1.2.2.2	Calcium-activated potassium channels (K _{Ca})	37
1.2.2.3	Inward rectifier potassium channel (K _{IR})	39
1.2.2.4	ATP-sensitive potassium channels (K _{ATP})	39
1.2.2.5	Transient outward current potassium channels (K _{to})	40
1.2.3	Chloride channels	40
1.2.4	Sodium channels	41
1.3	Cholinergic transmission	42
1.3.1	Cholinergic neurons	42
1.3.2	Cholinergic receptors (cholinoceptors)	42
1.3.2.1	Muscarinic receptors	43
1.3.2.1.a	Location of muscarinic receptors	43
1.3.2.1.b	Mechanisms of muscarinic receptors signal transduction	43
1.3.2.2	Nicotinic receptors	44
1.3.2.2.a	Locations of nicotinic receptors	44
1.3.2.2.b	Mechanisms of nicotinic receptors signal transduction	44
1.3.3	Characteristics of cholinergic transmission at various sites	45

1.3.3.1	Skeletal muscle	45
1.3.3.2	Autonomic ganglia	45
1.3.3.3	Autonomic effectors	45
1.3.3.3.a	Cardiovascular system	45
1.3.3.3.b	Gastrointestinal and urinary tracts	47
1.3.3.3.c	Miscellaneous effects	48
1.3.4	Cholinergic agonists and antagonists	48
1.4	Adrenergic transmission	50
1.4.1	Adrenergic neurons	50
1.4.2	Adrenergic receptors (adrenoceptors)	50
1.4.2.1	α -adrenergic receptors	50
1.4.2.1.a	Locations of α -adrenergic receptors	51
1.4.2.1.b	Mechanisms of α -adrenoceptors signal transduction	52
1.4.2.2	β -adrenergic receptors	52
1.4.2.2.a	Locations of β -adrenergic receptors	52
1.4.2.2.b	Mechanisms of β -adrenoceptors signal transduction	53
1.4.3	Characteristics of adrenergic transmission at various sites	53
1.4.3.1	Smooth muscle	53
1.4.3.2	Nerve terminals	54
1.4.3.3	Heart	54
1.4.3.4	Metabolism	54
1.4.4	Adrenergic agonists and antagonists	55
1.5	Hypertension	57
1.5.1	Drugs used in the treatment of hypertension	58
1.6	Endothelial dysfunction and oxidative stress in cardiovascular disease	60
1.7	Herbal medicine	62
1.7.1	History	62
1.7.2	Major clinical applications	63
1.8	Methods in phytochemical analysis	65
1.8.1	Methods of separation and identification	65
1.8.1.1	Thin layer chromatography (TLC)	66
1.8.1.2	Column chromatography (CC)	67
1.8.1.3	High-performance liquid chromatography (HPLC)	67
1.8.1.4	Infrared spectrophotometry	69
1.8.1.5	Ultraviolet spectrophotometry	70
1.9	<i>Loranthus ferrugineus</i> Roxb.	71
1.9.1	Taxonomy	72

1.10	Summary of the literature review, rationales of the thesis and research objectives	72
CHAPTER TWO – MATERIALS AND METHODS		74
2.1	List of tools and equipments	74
2.2	List of chemicals	75
2.3	Plant materials	77
2.4	Preparation of crude extracts	78
2.5	Experimental animals	81
2.6	Cardiovascular activities of <i>L. ferrugineus</i> extracts	81
2.6.1	Preparation of isolated rat thoracic aorta <i>in vitro</i>	81
2.6.1.1	Effects of <i>L. ferrugineus</i> extracts on isolated rat aortic ring preparations and comparison to standard drugs <i>in vitro</i>	83
2.6.1.1.a	Stability of isolated rat aortic ring preparations	83
2.6.1.1.b	Effects of solubilizing agents on isolated rat aortic ring preparations <i>in vitro</i>	84
2.6.1.1.c	Effects of phentolamine, verapamil and papaverine on noradrenaline-induced aortic rings contraction <i>in vitro</i>	84
2.6.1.1.d	Effects of <i>L. ferrugineus</i> extracts on noradrenaline-induced aortic rings contraction <i>in vitro</i>	85
2.6.2	Preparation of rat blood pressure <i>in vivo</i>	85
2.6.2.1	Effects of <i>L. ferrugineus</i> extracts on blood pressure of anesthetized rat <i>in vivo</i>	86
2.6.3	Preparation of isolated guinea pig ileum <i>in vitro</i>	88
2.6.3.1	Effects of <i>L. ferrugineus</i> methanol extract (LFME) on isolated guinea pig ileum preparations <i>in vitro</i>	89
2.7	Fractionation of LFME	90
2.8	Cardiovascular activities of LFME fractions	92
2.8.1	Effects of LFME fractions on blood pressure of anesthetized rat <i>in vivo</i>	92
2.8.2	Effects of LFME fractions on isolated rat aortic ring preparations <i>in vitro</i>	92
2.8.2.1	Effects of <i>n</i> -butanol fraction of <i>L. ferrugineus</i> methanol extract (NBF-LFME) on isolated rat aortic ring preparations <i>in vitro</i>	92
2.8.2.2	Effects of NBF-LFME on isolated guinea pig ileum preparations <i>in vitro</i>	95
2.9	Calculation of responses	95
2.9.1	<i>In vitro</i> experiments	95
2.9.2	<i>In vivo</i> experiments	96
2.10	Drugs and solutions	96

2.10.1	<i>In vitro</i> experiments	96
2.10.2	<i>In vivo</i> experiments	97
2.11	Termination of the experiments	97
2.12	Statistical analysis	97
2.13	Preliminary phytochemical screening	98
2.14	Determination of total phenolic content	99
2.15	Determination of total flavonoid content	100
2.16	DPPH assay	100
2.17	Assessment of total antioxidant activity	101
2.18	Column chromatography of NBF-LFME	101
2.19	Ultraviolet-Visible (UV-Vis) spectroscopy of LFME, NBF-LFME and NBF-LFME subfraction	103
2.20	Fourier transform infrared (FT-IR) spectroscopy of LFME, NBF-LFME and NBF-LFME subfraction	103
2.21	Qualitative HPLC analysis LFME, NBF-LFME and NBF-LFME subfraction	103
CHAPTER THREE – RESULTS		104
3.1	Cardiovascular activities of <i>L. ferrugineus</i> extracts	104
3.1.1	Effects of <i>L. ferrugineus</i> extracts on isolated rat aortic ring preparations and comparison to standard drugs <i>in vitro</i>	104
3.1.1.1	Stability of isolated rat aortic ring preparations	104
3.1.1.2	Effects of solubilizing agents on isolated rat aortic ring preparations <i>in vitro</i>	104
3.1.1.3	Effects of phentolamine, verapamil and papaverine on noradrenaline-induced aortic rings contraction <i>in vitro</i>	105
3.1.1.4	Effects of <i>L. ferrugineus</i> extracts on noradrenaline-induced aortic rings contraction <i>in vitro</i>	106
3.1.2	Effects of <i>L. ferrugineus</i> extracts on blood pressure of anesthetized rat <i>in vivo</i>	108
3.1.3	Effects of <i>L. ferrugineus</i> methanol extract (LFME) on isolated guinea pig ileum preparations <i>in vitro</i>	111
3.2	Cardiovascular activities of LFME fractions	112
3.2.1	Effects of LFME fractions on blood pressure of anesthetized rat <i>in vivo</i>	112
3.2.2	Effects of LFME fractions on isolated rat aortic ring preparations <i>in vitro</i>	112
3.2.3	Effects of <i>n</i> -butanol fraction of <i>L. ferrugineus</i> methanol extract (NBF-LFME) on isolated rat aortic ring preparations <i>in vitro</i>	113
3.2.4	Effects of NBF-LFME on isolated guinea pig ileum preparations <i>in vitro</i>	118

3.3	Phytochemistry results	169
3.3.1	Yield of <i>L. ferrugineus</i> extracts	169
3.3.2	Yield of LFME fractions	169
3.3.3	Phytochemical screening	170
3.3.4	Chemical assays on LFME and its fractions	179
3.3.5	Ultraviolet-Visible (UV-Vis) spectroscopy of LFME, NBF-LFME and NBF-LFME subfraction	179
3.3.6	Fourier transform infrared (FT-IR) spectroscopy of LFME, NBF-LFME and NBF-LFME subfraction	181
3.3.7	Qualitative HPLC analysis of LFME, NBF-LFME and NBF-LFME subfraction	184
3.3.8	Thin layer chromatography of NBF-LFME subfraction	186
CHAPTER FOUR – DISCUSSION		187
4.1	Animals and experimental design	188
4.2	Effects of <i>L. ferrugineus</i> extracts on isolated rat aortic ring preparations <i>in vitro</i>	193
4.3	Effects of <i>L. ferrugineus</i> extracts on blood pressure of anesthetized rat <i>in vivo</i> and possible mechanism(s) of action	198
4.4	Effects of LFME on isolated guinea pig ileum preparations <i>in vitro</i> and possible mechanism(s) of action	204
4.5	<i>In vivo</i> and <i>in vitro</i> activity screening of LFME fractions	205
4.6	Effects of NBF-LFME on isolated rat aortic ring preparations <i>in vitro</i> and possible mechanism(s) of action	206
4.7	Effects of NBF-LFME on isolated guinea pig ileum preparations <i>in vitro</i> and possible mechanism(s) of action	212
4.8	Phytochemistry of <i>L. ferrugineus</i>	214
CHAPTER FIVE – SUMMARY AND CONCLUSIONS		219
BIBLIOGRAPHY		222
APPENDICES		
LIST OF PUBLICATIONS		

LIST OF TABLES

		Page
Table 3.1	Effects of phentolamine, verapamil and papaverine on the median effective concentration (EC_{50}) and maximum response (R_{max}) of noradrenaline-induced contraction in isolated rat aortic ring preparations	161
Table 3.2	Effect of different extracts obtained from <i>L. ferrugineus</i> on maximum response (R_{max}) of noradrenaline-induced contraction in isolated rat aortic ring preparations	162
Table 3.3	Changes in the mean arterial blood pressure basal values before and after intravenous administration of antagonists	163
Table 3.4	Overall mean changes in the percentage of reduction or increase in mean arterial pressure and the duration of action of agonists or <i>L. ferrugineus</i> methanol extract in the presence of different antagonists	164
Table 3.5	Overall changes in the percentage of reduction in mean arterial blood pressure and duration of action of different fractions obtained from the methanol extract of <i>L. ferrugineus</i>	165
Table 3.6	Effect of different fractions obtained from the methanol extract of <i>L. ferrugineus</i> on the maximum relaxation response (R_{max}) on phenylephrine (1 μ M) and potassium chloride (80 mM)-precontracted isolated rat aortic ring preparations with intact endothelium	165
Table 3.7	Values of the median effective concentration (EC_{50}) and maximum relaxation (R_{max}) of <i>n</i> -butanol fraction of <i>L. ferrugineus</i> methanol extract in isolated rat aortic rings pretreated with various antagonists	166
Table 3.8	Values of the median effective concentration (EC_{50}) and maximum contraction (R_{max}) of calcium in the potassium chloride (KCl, 80 mM)-depolarized isolated rat aortic ring preparations with intact endothelium pretreated with either verapamil or <i>n</i> -butanol fraction of <i>L. ferrugineus</i> methanol extract	167
Table 3.9	Values of the median effective concentration (EC_{50}) and maximum contraction (R_{max}) of acetylcholine, <i>L. ferrugineus</i> methanol extract and <i>n</i> -butanol fraction of <i>L. ferrugineus</i> methanol extract in isolated guinea pig ileum pretreated with atropine	168
Table 3.10	Summary of the yields of the extracts obtained from the hot extraction of <i>L. ferrugineus</i>	169
Table 3.11	Summary of the yields of the fractions obtained from <i>L. ferrugineus</i> methanol extract	169

Table 3.12	Summary of the results obtained from <i>L. ferrugineus</i> methanol extract and <i>n</i> -butanol fraction of <i>L. ferrugineus</i> methanol extract chromatogram following spraying by sulfuric acid, heating and detection under visible light	170
Table 3.13	Summary of the results obtained from <i>L. ferrugineus</i> methanol extract and <i>n</i> -butanol fraction of <i>L. ferrugineus</i> methanol extract chromatogram following spraying by 0.5% anisaldehyde reagent and detection under visible and long-wave (365 nm) ultraviolet light	171
Table 3.14	Summary of the results obtained from <i>L. ferrugineus</i> methanol extract and <i>n</i> -butanol fraction of <i>L. ferrugineus</i> methanol extract chromatogram after spraying by 10% antimony trichloride in chloroform followed by heating at 100 °C for 5–6 min and detection under long-wave (365 nm) ultraviolet light	172
Table 3.15	Summary of the results obtained from <i>L. ferrugineus</i> methanol extract and <i>n</i> -butanol fraction of <i>L. ferrugineus</i> methanol extract chromatogram after spraying by 1% diphenylboric acid 2-aminoethyl ester in methanol followed by 5% polyethylene glycol 4000 in 96% ethanol and detection under long-wave (365 nm) ultraviolet light	173
Table 3.16	Summary of the results obtained from <i>L. ferrugineus</i> methanol extract and <i>n</i> -butanol fraction of <i>L. ferrugineus</i> methanol extract chromatogram following spraying by 5% aqueous ferric chloride solution and detection under visible light	175
Table 3.17	Summary of the results obtained from <i>L. ferrugineus</i> methanol extract and <i>n</i> -butanol fraction of <i>L. ferrugineus</i> methanol extract chromatogram after spraying by 20% aqueous sodium carbonate followed by Folin-Ciocalteu reagent and detection under visible light	176
Table 3.18	Chemical assays on <i>L. ferrugineus</i> methanol extract and its fractions	179
Table 3.19	FT-IR spectra for <i>L. ferrugineus</i> methanol extract, <i>n</i> -butanol fraction of <i>L. ferrugineus</i> methanol extract and the subfraction of <i>n</i> -butanol fraction of <i>L. ferrugineus</i> methanol extract	183

LIST OF FIGURES

		Page
Figure 1.1	The systemic and pulmonary circulation	2
Figure 1.2	Diagrammatic section of the heart	4
Figure 1.3	The cardiac action potential waveforms in adult human	7
Figure 1.4	Diagrammatic section of the blood vessel	9
Figure 1.5	Current scheme for endothelium-dependent relaxation	16

Figure 1.6	Mechanisms of vasorelaxation induced by nitric oxide	18
Figure 1.7	Reactions of superoxide anion with superoxide dismutase and nitric oxide	23
Figure 1.8	Regulation of smooth muscle contraction	32
Figure 1.9	Regulation of smooth muscle relaxation	33
Figure 1.10	<i>Loranthus ferrugineus</i> Roxb.	71
Figure 2.1	Soxhlet extractor	79
Figure 2.2	Reflux apparatus	79
Figure 2.3	Schematic diagram for preparation of <i>L. ferrugineus</i> crude extracts	80
Figure 2.4	Tissue organ bath	82
Figure 2.5	Grass polygraph model 79D (Quincy, Mass., USA)	83
Figure 2.6	Animal surgical preparation	86
Figure 2.7	Schematic diagram of fractionation of <i>L. ferrugineus</i> methanol extract	91
Figure 3.1	Repetitive concentration-response curve of noradrenaline-induced contractile response in isolated rat aortic ring preparations	119
Figure 3.2	Effect of polyethylene glycol 400 on noradrenaline-induced contraction of isolated rat aortic ring preparations	120
Figure 3.3	Effect of dimethylsulfoxide on noradrenaline-induced contraction of isolated rat aortic ring preparations	121
Figure 3.4	Effect of phentolamine on noradrenaline-induced contractile response in isolated rat aortic ring preparations	122
Figure 3.5	Effect of verapamil on noradrenaline-induced contractile response in isolated rat aortic ring preparations	123
Figure 3.6	Effect of papaverine on noradrenaline-induced contractile response in isolated rat aortic ring preparations	124
Figure 3.7	Effect of <i>L. ferrugineus</i> petroleum ether extract on noradrenaline-induced contractile response in isolated rat aortic ring preparations	125
Figure 3.8	The effect of <i>L. ferrugineus</i> chloroform extract on noradrenaline-induced contractile response in isolated rat aortic ring preparations	126
Figure 3.9	Effect of <i>L. ferrugineus</i> ethyl acetate extract on noradrenaline-induced contractile response in isolated rat aortic ring preparations	127
Figure 3.10	Effect of <i>L. ferrugineus</i> methanol extract on noradrenaline-induced contractile response in isolated rat aortic ring preparations	128

Figure 3.11	Effect of <i>L. ferrugineus</i> water extract on noradrenaline-induced contractile response in isolated rat aortic ring preparations	129
Figure 3.12	Percent reduction in mean arterial pressure elicited by i.v. injection of increasing doses of <i>L. ferrugineus</i> petroleum ether, chloroform, ethyl acetate, methanol and water extracts in anesthetized Sprague Dawley rats	130
Figure 3.13	Effect of i.v. pretreatment with atropine on percent reduction in mean arterial pressure elicited by i.v. injection of increasing doses of acetylcholine and <i>L. ferrugineus</i> methanol extract in anesthetized Sprague Dawley rats	131
Figure 3.14	Effect of i.v. pretreatment with neostigmine on percent reduction in mean arterial pressure elicited by i.v. injection of increasing doses of acetylcholine and <i>L. ferrugineus</i> methanol extract in anesthetized Sprague Dawley rats	132
Figure 3.15	Effect of i.v. pretreatment with neostigmine on duration of action elicited by i.v. injection of increasing doses of acetylcholine and <i>L. ferrugineus</i> methanol extract in anesthetized Sprague Dawley rats	133
Figure 3.16	Effect of i.v. pretreatment with hexamethonium on percent change in mean arterial pressure elicited by i.v. injection of increasing doses of nicotine and <i>L. ferrugineus</i> methanol extract in anesthetized Sprague Dawley rats	134
Figure 3.17	Effect of i.v. pretreatment with L-NAME on percent reduction in mean arterial pressure elicited by i.v. injection of increasing doses of acetylcholine and <i>L. ferrugineus</i> methanol extract in anesthetized Sprague Dawley rats	135
Figure 3.18	Effect of i.v. pretreatment with L-NAME on duration of action elicited by i.v. injection of increasing doses of acetylcholine and <i>L. ferrugineus</i> methanol extract in anesthetized Sprague Dawley rats	136
Figure 3.19	Effect of i.v. pretreatment with propranolol on percent reduction in mean arterial pressure elicited by i.v. injection of increasing doses of isoprenaline and <i>L. ferrugineus</i> methanol extract in anesthetized Sprague Dawley rats	137
Figure 3.20	Effect of i.v. pretreatment with prazosin on percent change in mean arterial pressure elicited by i.v. injection of increasing doses of noradrenaline and <i>L. ferrugineus</i> methanol extract in anesthetized Sprague Dawley rats	138
Figure 3.21	Effects of atropine on the contractile responses induced by increasing concentrations of acetylcholine and <i>L. ferrugineus</i> methanol extract in isolated guinea pig ileum preparations	139

Figure 3.22	Typical tracers of acetylcholine-induced contractile response in isolated guinea pig ileum: (A) without pretreatment, (B) with 1 μ M atropine pretreatment, (C) with 0.05 μ M neostigmine pretreatment and (D) with 100 μ M hexamethonium pretreatment, and <i>L. ferrugineus</i> methanol extract-induced contractile response in isolated guinea pig ileum: (E) without pretreatment, (F) with 1 μ M atropine pretreatment, (G) with 0.05 μ M neostigmine pretreatment and (H) with 100 μ M hexamethonium pretreatment	140
Figure 3.23	The effects of i.v. injection of increasing doses of chloroform, ethyl acetate, <i>n</i> -butanol and water fractions of <i>L. ferrugineus</i> methanol extract on percent reduction in mean arterial pressure and duration of action in anesthetized Sprague Dawley rats	141
Figure 3.24	The effects of i.v. injection of increasing doses of <i>L. ferrugineus</i> methanol extract and its <i>n</i> -butanol fraction on percent reduction in mean arterial pressure in anesthetized Sprague Dawley rats	142
Figure 3.25	Vasodilatation effects of <i>n</i> -butanol fraction of <i>L. ferrugineus</i> methanol extract, water fraction of <i>L. ferrugineus</i> methanol extract, chloroform fraction of <i>L. ferrugineus</i> methanol extract and ethyl acetate fraction of <i>L. ferrugineus</i> methanol extract on 1 μ M phenylephrine-precontracted endothelium-intact isolated rat aortic ring preparations	143
Figure 3.26	Vasodilatation effects of <i>n</i> -butanol fraction of <i>L. ferrugineus</i> methanol extract, water fraction of <i>L. ferrugineus</i> methanol extract, chloroform fraction of <i>L. ferrugineus</i> methanol extract and ethyl acetate fraction of <i>L. ferrugineus</i> methanol extract on 80 mM potassium chloride-precontracted endothelium-intact isolated rat aortic ring preparations	144
Figure 3.27	Vasodilatation effect of <i>n</i> -butanol fraction of <i>L. ferrugineus</i> methanol extract vs. vehicle (Kreb's solution) on 1 μ M phenylephrine-precontracted endothelium-intact isolated rat aortic ring preparations	145
Figure 3.28	Vasodilatation effect of <i>n</i> -butanol fraction of <i>L. ferrugineus</i> methanol extract on 1 μ M phenylephrine-precontracted endothelium-intact and -denuded isolated rat aortic ring preparations	146
Figure 3.29	Vasodilatation effect of <i>n</i> -butanol fraction of <i>L. ferrugineus</i> methanol extract on 1 μ M phenylephrine-precontracted vs. 80 mM potassium chloride-precontracted endothelium-intact isolated rat aortic ring preparations	147
Figure 3.30	Vasodilatation effect of <i>n</i> -butanol fraction of <i>L. ferrugineus</i> methanol extract on 1 μ M phenylephrine-precontracted endothelium-intact rat aortic ring preparations incubated with atropine	148
Figure 3.31	Vasodilatation effect of <i>n</i> -butanol fraction of <i>L. ferrugineus</i> methanol extract on 1 μ M phenylephrine-precontracted endothelium-intact rat aortic ring preparations incubated with L-NAME	149
Figure 3.32	Vasodilatation effect of <i>n</i> -butanol fraction of <i>L. ferrugineus</i> methanol extract on 1 μ M phenylephrine-precontracted endothelium-intact rat aortic ring preparations incubated with methylene blue	150

Figure 3.33	Vasodilatation effect of <i>n</i> -butanol fraction of <i>L. ferrugineus</i> methanol extract on 1 μ M phenylephrine-precontracted endothelium-intact rat aortic ring preparations incubated with indomethacin	151
Figure 3.34	Vasodilatation effect of <i>n</i> -butanol fraction of <i>L. ferrugineus</i> methanol extract on 1 μ M phenylephrine-precontracted endothelium-intact rat aortic ring preparations incubated with glibenclamide	152
Figure 3.35	Vasodilatation effect of <i>n</i> -butanol fraction of <i>L. ferrugineus</i> methanol extract on 1 μ M phenylephrine-precontracted endothelium-intact rat aortic ring preparations incubated with propranolol	153
Figure 3.36	Vasodilatation effect of <i>n</i> -butanol fraction of <i>L. ferrugineus</i> methanol extract on 80 mM potassium chloride-precontracted endothelium-intact rat aortic ring preparations incubated with prazosin	154
Figure 3.37	Effect of verapamil on calcium induced-contraction of 80 mM potassium chloride-depolarized endothelium-intact isolated rat aortic ring preparations	155
Figure 3.38	Effect of <i>n</i> -butanol fraction of <i>L. ferrugineus</i> methanol extract on calcium-induced contraction of 80 mM potassium chloride-depolarized endothelium-intact isolated rat aortic ring preparations	156
Figure 3.39	Effect of cumulative additions of acetylcholine on relaxation response on 1 μ M phenylephrine-precontracted endothelium-intact rat aortic ring preparations incubated with <i>n</i> -butanol fraction of <i>L. ferrugineus</i> methanol extract	157
Figure 3.40	Effect of cumulative additions of sodium nitroprusside on relaxation response on 1 μ M phenylephrine-precontracted endothelium-denuded rat aortic ring preparations incubated with <i>n</i> -butanol fraction of <i>L. ferrugineus</i> methanol extract	158
Figure 3.41	Effect of atropine on the contractile response induced by increasing concentrations of <i>n</i> -butanol fraction of <i>L. ferrugineus</i> methanol extract in isolated guinea pig ileum preparations	159
Figure 3.42	Typical tracers of <i>n</i> -butanol fraction of <i>L. ferrugineus</i> methanol extract-induced contractile response in isolated guinea pig ileum: (A) without pretreatment, (B) with 1 μ M atropine pretreatment, (C) with 0.05 μ M neostigmine pretreatment and (D) with 100 μ M hexamethonium pretreatment	170
Figure 3.43	TLC profile of <i>L. ferrugineus</i> methanol extract and its <i>n</i> -butanol fraction using chloroform: methanol (3:17 v/v) as mobile phase and sulfuric acid as spraying reagent followed by heating at 105 $^{\circ}$ C for 5 min	171
Figure 3.44	TLC profile of <i>L. ferrugineus</i> methanol extract and its <i>n</i> -butanol fraction using chloroform: methanol (3:17 v/v) as mobile phase and 0.5% anisaldehyde in sulfuric acid, glacial acetic acid and methanol as spraying reagent followed by heating at 100 $^{\circ}$ C for 5–10 min.	172

Figure 3.45	TLC profile of <i>L. ferrugineus</i> methanol extract and its <i>n</i> -butanol fraction using chloroform: methanol (3:17 v/v) as mobile phase and 10% antimony trichloride in chloroform as spraying reagent followed by heating at 100 °C for 5–6 min	173
Figure 3.46	TLC profile of <i>L. ferrugineus</i> methanol extract and its <i>n</i> -butanol fraction using chloroform: methanol (3:17 v/v) as mobile phase and 1% diphenylboric acid 2-aminoethyl ester in methanol followed by 5% polyethylene glycol 4000 in 96% ethanol as spraying reagents	174
Figure 3.47	TLC profile of <i>L. ferrugineus</i> methanol extract and its <i>n</i> -butanol fraction using chloroform: methanol (3:17 v/v) as mobile phase and 5% aqueous ferric chloride solution as spraying reagent	175
Figure 3.48	TLC profile of <i>L. ferrugineus</i> methanol extract and its <i>n</i> -butanol fraction using chloroform: methanol (3:17 v/v) as mobile phase and 20% aqueous sodium carbonate followed by Folin-Ciocalteu reagent as spraying reagent	177
Figure 3.49	Froth formations following the performance of foam test on <i>L. ferrugineus</i> methanol extract and its <i>n</i> -butanol fraction	177
Figure 3.50	Tannins precipitation test in an aqueous solution of either <i>L. ferrugineus</i> methanol extract or its <i>n</i> -butanol fraction before and after the addition of 10% lead acetate solution	179
Figure 3.51	UV spectrum of <i>L. ferrugineus</i> methanol extract	179
Figure 3.52	UV spectrum of <i>n</i> -butanol fraction of <i>L. ferrugineus</i> methanol extract	180
Figure 3.53	UV spectrum of the subfraction of <i>n</i> -butanol fraction of <i>L. ferrugineus</i> methanol extract	181
Figure 3.54	FT-IR spectrum of <i>L. ferrugineus</i> methanol extract	181
Figure 3.55	FT-IR spectrum of <i>n</i> -butanol fraction of <i>L. ferrugineus</i> methanol extract	182
Figure 3.56	FT-IR spectrum of the subfraction of <i>n</i> -butanol fraction of <i>L. ferrugineus</i> methanol extract	183
Figure 3.57	HPLC profile of <i>L. ferrugineus</i> methanol extract	183
Figure 3.58	HPLC profile of <i>n</i> -butanol fraction of <i>L. ferrugineus</i> methanol extract	184
Figure 3.59	HPLC profile of the subfraction of <i>n</i> -butanol fraction of <i>L. ferrugineus</i> methanol extract	185
Figure 3.60	TLC profile of the subfraction of <i>n</i> -butanol fraction of <i>L. ferrugineus</i> methanol extract using <i>n</i> -butanol: acetic acid: water (5:1:4 v/v)	186

LIST OF ABBREVIATIONS

°C	Degree celsius
λ	Lambda
%	Percent
±	Plus minus
20-HETE	20-hydroxyeicosatetraenoic acid
5-HT	5-hydroxy tryptamine
AA	Arachidonic acid
ACE	Angiotensin-converting enzyme
ACEI	Angiotensin-converting enzyme inhibitor
Ach	Acetylcholine
AChE	Acetylcholinesterase
Ang	Angiotensin
ANOVA	Analysis of variance
ANP	Arterial natriuretic peptide
AT-1	Angiotensin type I receptor
ATP	Adenosine triphosphate
AV	Atrioventricular
BK _{Ca}	Large-conductance calcium-sensitive potassium channel
BP	Blood pressure
BPH	Benign prostatic hyperplasia
BRNs	Baroreceptor neurons
Ca ²⁺	Calcium ion
cAMP	Cyclic adenosine monophosphate
CC	Column chromatography
CF-LFME	Chloroform fraction of <i>Loranthus ferrugineus</i> methanol extract
cGMP	Cyclic guanosine monophosphate
CHD	Coronary heart disease
CHF	Congestive heart failure
ChTX	Charybdotoxin
Cl ⁻	Chloride ion
Cl _{Ca}	Calcium-activated chloride channel
Cl _{VR}	Volume-regulated chloride channel
cm	Centimeter
CNS	Central nervous system
CO	Cardiac output
COMT	Catechol O-methyl transferase
COX	Cyclooxygenase
CVD	Cardiovascular disease
CVP	Central venous pressure
d	Day
DAG	Diacylglycerol
DBP	Diastolic blood pressure
DMPP	1,1-dimethyl-4-phenylpiperazinium iodide
DMSO	Dimethylsulfoxide
EAF-LFME	Ethyl acetate fraction of <i>Loranthus ferrugineus</i> methanol extract
EC ₅₀	Median effective concentration
ecSOD	Extracellular superoxide dismutase
EDCF	Endothelium-derived contracting factor
EDHF	Endothelium-derived hyperpolarizing factor
EDRF	Endothelium-derived relaxation factor

EET	Epoxyeicosatrienoic acid
eNOS	Endothelial nitric oxide synthase
ENS	Enteric nervous system
ET	Endothelin
<i>et al.</i>	And others
ETA	Endothelin receptor A
ETB	Endothelin receptor B
F	Flow
FTIR	Fourier transform infrared
g	Gram
GCP	Good clinical practice
GIT	Gastrointestinal tract
h	Hour
H ₂ O ₂	Hydrogen peroxide
HbO ₂	Oxyhemoglobin
HO [•]	Hydroxyl radical
HOCl	Hypochlorous acid
HPLC	High-performance liquid chromatography
HVA	High voltage-activated
i.p.	Intraperitoneal
i.u.	International unit
i.v.	Intravenous
IbTX	Iberiotoxin
IK _{Ca}	Intermediate-conductance calcium-sensitive potassium channel
iNOS	Inducible nitric oxide synthase
IP	PGI ₂ receptor
IP ₃	1,4,5-inositoltriphosphate
IR	Infrared
IRAG	1,4,5-inositoltriphosphate receptor associated cGMP kinase substrate
ISP	Isoprenaline
K ⁺	Potassium ion
K _{ATP}	ATP-sensitive potassium channel
K _{Ca}	Calcium-activated potassium channel
kg	Kilogram
K _{IR}	Inward rectifier potassium channel
K _{to}	Transient outward current K ⁺ channel
K _V	Delayed rectifier potassium channel
L	Liter
LFCE	<i>Loranthus ferrugineus</i> chloroform extract
LFEEAE	<i>Loranthus ferrugineus</i> ethyl acetate extract
LFME	<i>Loranthus ferrugineus</i> methanol extract
LFPEE	<i>Loranthus ferrugineus</i> petroleum ether extract
LFWE	<i>Loranthus ferrugineus</i> water extract
L-NAME	N ^o -nitro-L-arginine methyl ester
L-NIO	N-iminoethyl-L-ornithine
L-NMMA	N ^G -monomethyl-L-arginine
LVA	Low voltage-activated
m	Meter
μg	Microgram
μL	Microliter
μM	Micromolar
μm	Micrometer
M	Molar
MAP	Mean arterial pressure
mg	Milligram
MI	Myocardial infarction

min	Minute
mL	Milliliter
MLC	Myosin light chain
mm	Millimeter
mM	Millimolar
MS	Mass spectroscopy
mV	Millivolt
MW	Molecular weight
n	Number of determination
Na ⁺	Sodium ion
NADH	Nicotinamide adenine dinucleotide
NADPH	Nicotinamide adenine dinucleotide phosphate
NBF-LFME	<i>n</i> -butanol fraction of <i>Loranthus ferrugineus</i> methanol extract
NA	Noradrenaline
NFκB	Nuclear factor κb
NMR	Nuclear magnetic resonance
nNOS	Neuronal nitric oxide synthase
NO	Nitric oxide
NO [•]	Nitric oxide radical
NOS	Nitric oxide synthase
O ₂ ^{-•}	Superoxide anion
ONOO ⁻	Peroxynitrite
ONOOCO ₂ ⁻	Peroxynitrite carbonate adduct
P	Pressure
<i>P</i>	Probability
PDE	Phosphodiesterase
PE	Phenylephrine
PEG	Polyethylene glycol
PGI ₂	Prostacyclin
PIP ₂	Phosphatidyl inositol-(4,5)-biphosphate
PK	Protein kinase
PLC	Phospholipase C
PMS	Postmenstrual syndrome
pS	Petasiemens
PVR	Peripheral vascular resistance
R	Resistance
RAAS	Renin-angiotensin-aldosterone system
RAS	Renin-angiotensin system
R-COO [•]	Fatty acid peroxy radical
R _f	Retention factor
RhoGEF	Rho guanine nucleotide exchange factor
R _{max}	Maximum response
RNA	Ribonucleic acid
ROS	Reactive oxygen species
RSA	Radical scavenging activity
s	Second
S.E.M.	Standard error of mean
SA	Sinoatrial
SAC	Stretch-activated cation channel
SBP	Systolic blood pressure
SD	Sprague Dawley
SERCA	Sarcoplasmic reticulum ATPase
SK _{Ca}	Small-conductance calcium-sensitive potassium channel
SNP	Sodium nitroprusside
SNS	Sympathetic nervous system
SOC	Store-operated calcium channel

SOD	Superoxide dismutase
SVR	Systemic vascular resistance
TAA	Total antioxidant activity
TEA	Tetraethyl ammonium
TEAC	Trolox equivalent antioxidant capacity
TLC	Thin layer chromatography
TMA	Tetramethylammonium
TPR	Total peripheral resistance
TX	Thromboxane
TXA ₂	Thromboxane A ₂
UV	Ultraviolet
UV-Vis	Ultraviolet-Visible
v/v	Volume by volume
VCAM-1	Vascular cell adhesion molecule
vs.	Versus
VSM	Vascular smooth muscle
w/v	Weight by volume
w/w	Weight by weight
WF-LFME	Water fraction of <i>Loranthus ferrugineus</i> methanol extract

**AKTIVITI KARDIOVASKULAR EKSTRAK METANOL *LORANTHUS FERRUGINEUS*
ROXB. DAN FRAKSINYA**

ABSTRAK

Loranthus ferrugineus Roxb. ialah suatu tumbuhan renek hemiparasitik yang secara tradisionalnya digunakan untuk merawat hipertensi. Dalam kajian ini, fraksinasi berpandukan kesan kardiovaskular dilakukan sebagai percubaan untuk mengenalpasti fraksi aktif dan menentukan mekanisme tindakannya. Tumbuhan dikeringkan, diserbukkan dan diekstraksi berganti-ganti dengan eter petroleum, kloroform, etil asetat, metanol dan air. Setiap ekstrak dikeringkan dalam tekanan rendah dan disejukkan. Kesan setiap ekstrak dikaji ke atas sediaan terasing gelang aorta tikus dan tikus terbius. Ekstrak metanol (LFME) didapati paling poten dalam menyasarkan kelok log kepekatan gerakbalas noradrenalin (NA) ke kanan dengan penurunan gerak balas maksimum. Keputusan percubaan ini mencadangkan ekstrak bertindak sebagai perencat tak kompetitif kepada NA. LFME juga didapati paling poten dalam menurunkan tekanan darah tikus terbius. Sama seperti asetilkolina (Ach), prarawatan dengan atropina mengurangkan kesan penurunan tekanan darah oleh LFME dengan signifikan ($P < 0.05$) menyarankan LFME bertindak sebagai agonis kolinergik. Prarawatan dengan N ω -nitro-L-arginin metil ester (L-NAME, 10 mg/kg) mengurangkan tekanan arteri purata (MAP) tikus yang diaruhkan LFME dengan signifikan ($P < 0.05$). Sebaliknya, tidak berlaku perubahan yang signifikan ($P > 0.05$) dalam MAP setelah suntikan intra-vena neostigmin (40 μ g/kg), heksametonium (30 mg/kg), propranolol (2 mg/kg) dan prazosin (50 μ g/kg). Dengan cara ekstraksi pelarut-pelarut, LFME yang aktif difraksikan secara berturut dengan kloroform, etil asetat dan *n*-butanol. Kesan fraksi yang telah disejukkan kemudian dikaji ke atas sediaan tikus terbius. Di antara keempat-empat fraksi, fraksi *n*-butanol dari LFME (NBF-LFME) didapati menyebabkan penurunan tekanan darah yang paling besar dan paling lama. NBF-LFME (1.00E-5–3.00 mg/mL) juga menyebabkan perencatan yang paling besar pengecutan gelang aorta aruhan fenilefrina dan kepekatan tinggi K⁺. Pembuangan lapisan

endotelium dari gelang aorta menghapuskan sepenuhnya sifat mengendurkan vaskular NBF-LFME. Prarawatan dengan atropina (1 μM), L-NAME (10 μM), indometasin (10 μM) dan metilena biru (10 μM) menghalang dengan signifikan ($P < 0.001-0.05$) pengenduran yang diperantarakan NBF-LFME. NBF-LFME (0.05, 0.1 dan 0.3 mg/mL) tidak mengubah dengan signifikan ($P > 0.05$) kesan pengecutan bergantung kepekatan yang diaruhkan oleh penambahan kumulatif kalsium ($3.00\text{E}-03-3.00\text{E}-02\text{M}$) dalam kepekatan tinggi K^+ (80 mM) gelang aorta terdepolarisasi yang diinkubasikan di dalam larutan Krebs bebas kalsium. Pengenduran bergantung endotelium dan takbergantung endotelium aruhan Ach dan natrium nitroprusida (SNP), masing-masing, ditingkatkan dengan signifikan ($P < 0.001-0.05$) pada gelang aorta yang diprarawat dengan NBF-LFME (0.3 mg/mL). Sebaliknya, glibenklamida (10 μM), propranolol (1 μM) dan prazosin (0.01 μM) tidak mengubah ($P > 0.05$) pengenduran yang diaruhkan NBF-LFME. Pada sediaan ileum argus, NBF-LFME (0.065–4 mg/mL) mengaruhkan pengecutan bergantung kepekatan. Pengecutan ini direncat dengan signifikan ($P < 0.001$) oleh atropina (1 μM) tetapi dipotensiasikan oleh neostigmin (0.05 μM). Heksametonium (100 μM) tiada kesan ke atas pengecutan yang diaruhkan NBF-LFME. Hasil kajian mencadangkan *L. ferrugineus* mengaruhkan kesan kardiovaskularnya dengan merangsang reseptor muskarinik, mengaktifkan lintasan pengrehat nitrik oksida-cGMP terbitan endotelium, menggalakk dan pelepasan prostasiklin dan/atau mungkin melalui kemampuannya memanjangkan separuh-hayat nitrik oksida. Analisa kimia NBF-LFME menggunakan spektroskopi UV dan IR, kromatografi turus dan HPLC menunjukkan terdapatnya terpenoid dalam NBF-LFME.

**CARDIOVASCULAR ACTIVITIES OF *LORANTHUS FERRUGINEUS* ROXB.
METHANOL EXTRACT AND ITS FRACTIONS**

ABSTRACT

Loranthus ferrugineus Roxb. is a hemiparasitic shrub traditionally used for treatment of hypertension. In the present study, the cardiovascular effects-guided fractionation of *L. ferrugineus* was performed in an attempt to identify the active fraction and determine its mechanism of action. The plant was dried, pulverized and successively extracted with petroleum ether, chloroform, ethyl acetate, methanol and water. Each extract was dried under reduced pressure and freeze-dried. The effect of each extract was examined on isolated rat aortic ring and anesthetized rat preparations. The methanol extract (LFME) was found to be the most potent in shifting the log concentration response curve of noradrenaline (NA) to the right with reduced maximum response. It suggests that the extract acts as a non-competitive inhibitor to NA. The methanol extract was also found to be the most potent in lowering blood pressure of anesthetized rats. Similar to acetylcholine (Ach), pretreatment with atropine significantly ($P < 0.05$) decreased the blood pressure lowering effect of LFME which suggests that LFME acts as cholinergic agonist. Similarly, pretreatment with N ω -nitro-L-arginine methyl ester (L-NAME, 10 mg/kg) significantly ($P < 0.05$) inhibited the reduction in mean arterial pressure (MAP) induced by LFME. Conversely, no significant ($P > 0.05$) changes in MAP were seen following intravenous injections of neostigmine (40 μ g/kg), hexamethonium (30 mg/kg), propranolol (2 mg/kg) and prazosin (50 μ g/kg). By means of solvent-solvent extraction, the aqueous LFME solution was successively fractionated using chloroform, ethyl acetate and *n*-butanol. The effects of the freeze-dried fractions were then investigated in anesthetized rat preparation. Among the four fractions, the *n*-butanol fraction of LFME (NBF-LFME) was found to cause the largest and longest lowering of blood pressure. The NBF-LFME (1.00E-5–3.00 mg/mL) also caused the largest inhibition of phenylephrine (PE)- and high K⁺-induced aortic ring contraction. Removal of the endothelium of the aortic ring completely abolished the vascular

relaxing properties of NBF-LFME. Pretreatment with atropine (1 μM), L-NAME (10 μM), indomethacin (10 μM) and methylene blue (10 μM) significantly ($P < 0.001$ – 0.05) blocked NBF-LFME-mediated relaxation. NBF-LFME (0.05, 0.1 and 0.3 mg/mL) did not significantly ($P > 0.05$) alter the concentration-dependent contractile effect induced by cumulative additions of calcium ($3.00\text{E-}03$ – $3.00\text{E-}02\text{M}$) in high K^+ (80 mM) depolarized aortic rings incubated in calcium-free Krebs's solution. Endothelium-dependent and -independent relaxations induced by Ach and sodium nitroprusside (SNP), respectively, were significantly ($P < 0.001$ – 0.05) enhanced in aortic rings pretreated with NBF-LFME (0.3 mg/mL). On the contrary, glibenclamide (10 μM), propranolol (1 μM) and prazosin (0.01 μM) did not ($P > 0.05$) alter NBF-LFME-induced relaxation. In guinea-pig ileum preparation, NBF-LFME (0.065–4 mg/mL) induced concentration-dependent contraction. This contraction was significantly ($P < 0.001$) inhibited by atropine (1 μM) but potentiated by neostigmine (0.05 μM). Hexamethonium (100 μM) had no effect on NBF-LFME-induced contraction. The results suggest that *L. ferrugineus* induced its cardiovascular effects by stimulating cardiovascular muscarinic receptor, activating the endothelium-derived nitric oxide-cGMP-relaxant pathway, promoting prostacyclin release and/or possibly through its ability to lengthen the released nitric oxide half life. Chemical analysis of NBF-LFME using UV and IR spectroscopies, thin layer chromatography, column chromatography and HPLC indicated the presence of terpenoids in the NBF-LFME.

CHAPTER ONE**INTRODUCTION****1.1 The circulatory system****1.1.1 The systemic and pulmonary circulation**

A British physiologist, William Harvey, reported in 1628 that the cardiovascular system forms a closed loop so that blood pumped out of the heart through one set of vessels returns to the heart by a different set. There are in fact two circuits (Figure 1.1), both originating and terminating in the heart. The latter is divided longitudinally into two functional halves each of which contain two chambers: an upper chamber, the atrium, and a lower chamber, the ventricle. The atrium on each side empties into the ventricle on that side; yet, no direct flow between the two atria or the two ventricles in the heart of the adult is found (Widmaier *et al.*, 2006).

An eminent Arab physician, Ibn Al-Nafis, was the first to define the pulmonary circulation in the thirteenth century. Based on his report, it is now well accepted that in the pulmonary circulation the blood is pumped from the right ventricle through the lungs and then to the left atrium. From the left ventricle, it is then pumped through the systemic circulation and subsequently through all the organs and tissues of the body except the lungs, and then to the right atrium. In both circuits, the vessels transporting blood away from the heart are called arteries, and those carrying blood from body organs and tissues back to the heart are called veins (Al-Ghazal, 2007).

In the systemic circuit, blood leaves the left ventricle by a single huge artery, the aorta (Figure 1.1). From the aorta, the arteries of the systemic circulation branch off, dividing into increasingly smaller vessels, the smallest arteries branch into arterioles, which in turn branch into a large number (estimated at 10 billions) of exceedingly small vessels called capillaries, which fuse to form larger-diameter vessels, the venules. The arterioles, capillaries, and venules are together termed the microcirculation.

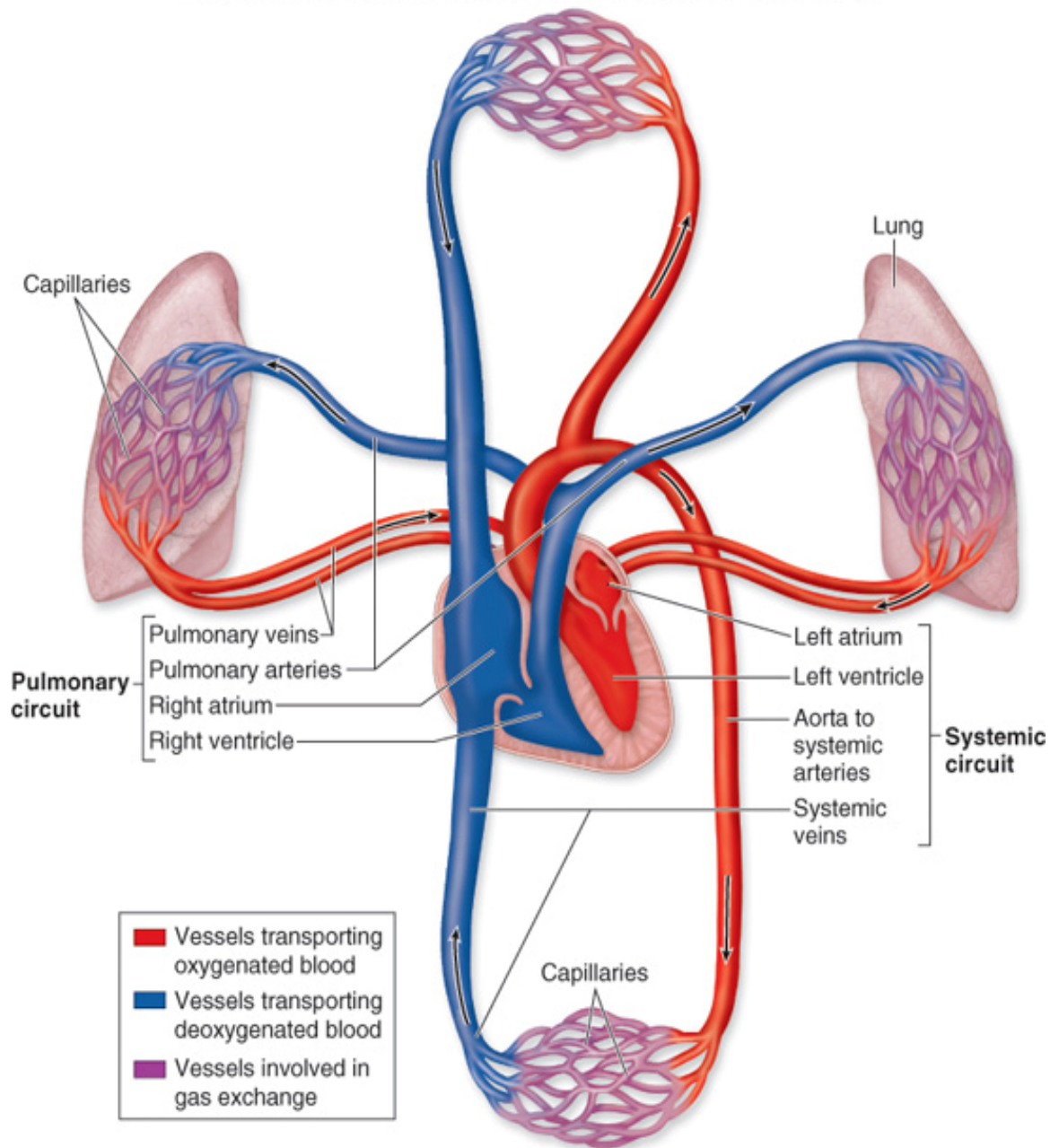


Figure 1.1: The systemic and pulmonary circulation. (Adapted from McKinley and O'Loughlin, 2007)

The venules in the systemic circulation then join to form larger vessels, the veins. Two large veins are formed when the veins from the various peripheral organs and tissues join together, the inferior vena cava, which accumulates blood from below the heart, and the superior vena cava, which collects blood from above the heart. These two main veins return the blood to the right atrium.

The pulmonary circulation is comprised of a comparable circuit. Through a single large artery known as the pulmonary trunk, blood leaves the right ventricle. This large artery further divides into the two pulmonary arteries, one supplying the right lung and the other the left. In the lungs, the arteries continue to divide, eventually forming capillaries that join into venules and then veins. The blood leaves the lungs via four pulmonary veins, which ultimately empty into the left atrium.

While blood flows through the lung capillaries, it picks up oxygen supplied to the lungs through breathing process. Therefore, high oxygen contents are found in the blood in the pulmonary veins, left side of the heart, and systemic arteries. As this blood flows through peripheral tissues and organs capillaries, some of this oxygen leaves the blood to be consumed by cells, resulting in the lower oxygen content of blood in the venous side of the systemic circulation.

Lastly, there are a number of exceptions, particularly the liver, kidneys, and pituitary, to the typical anatomical pattern described in this section for the systemic circulation. In those organs, blood is known to pass through two major capillary beds, arranged in series, before returning to the heart. This prototype is recognized as a portal system (Widmaier *et al.*, 2006).

1.1.2 The heart

1.1.2.1 Anatomy

The heart is a unique muscular organ enclosed in a fibrous sac, the pericardium, and located inside the chest (Figure 1.2). Another fibrous membrane is closely attached to the heart and is known as the epicardium. The very narrow space between the pericardium and epicardium is filled with a watery fluid that acts as a lubricant while the heart moves within the sac.

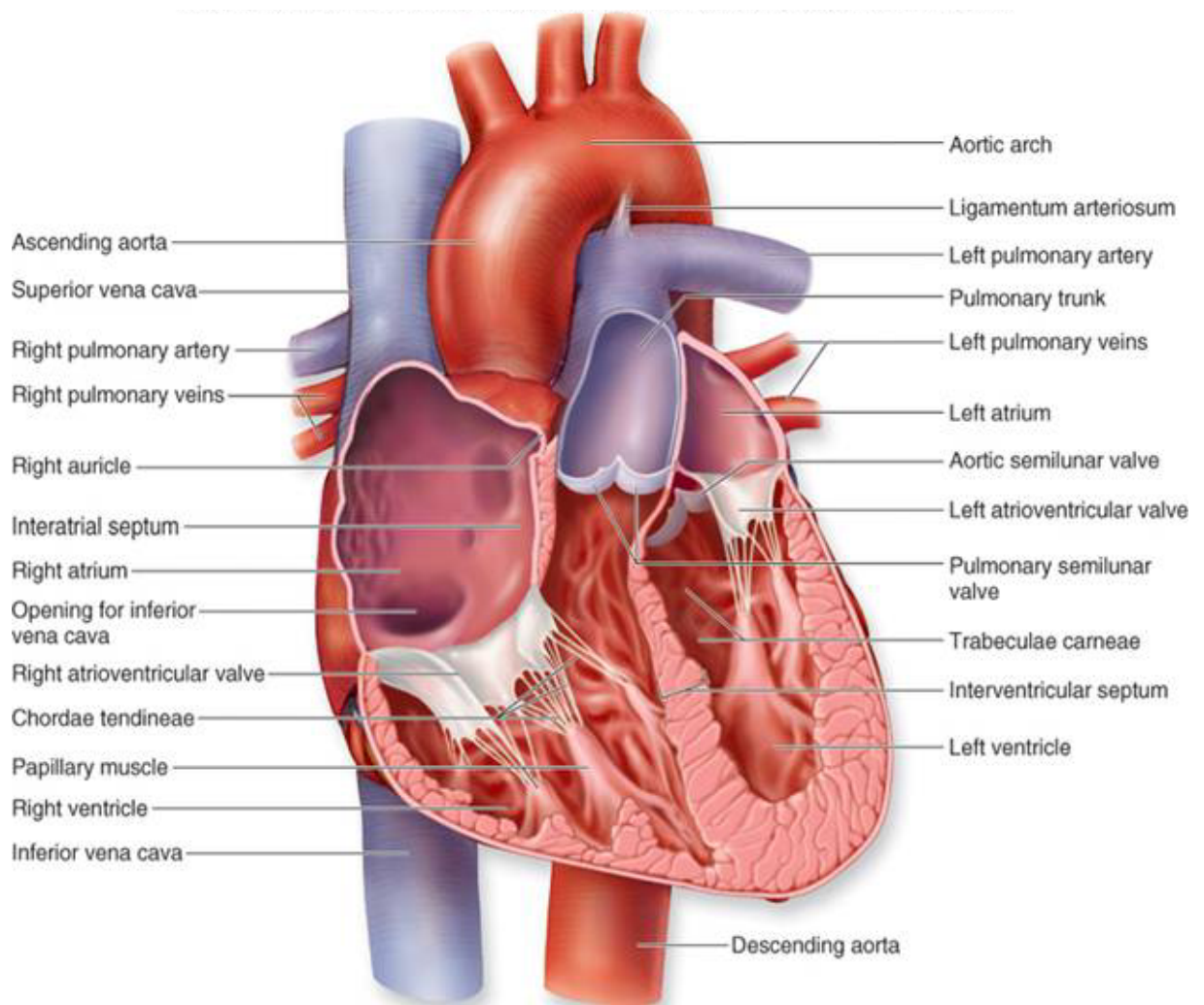


Figure 1.2: Diagrammatic section of the heart. (Adapted from McKinley and O'Loughlin, 2007)

The walls of the heart, the myocardium, are composed principally of cardiac muscle cells. The internal surface of the cardiac chamber, as well as the inner wall of all blood vessels, is lined by a thin layer of cells known as endothelial cells, or endothelium.

The heart is divided into right and left halves, each half consisting of an atrium and a ventricle. The two ventricles are separated by a muscular wall, the interventricular septum. Located between the atrium and ventricle in each half of the heart are the atrioventricular (AV) valves, which allow blood to flow from atrium to ventricle but not in the opposite direction. The right AV valve is called the tricuspid valve since it has three fibrous flaps, or cusps. The left AV valve has two flaps and is therefore called the bicuspid valve (its resemblance to a bishop's headgear has earned the left AV valve the frequently used name mitral valve).

The openings of the right ventricle into the pulmonary trunk and of the left ventricle into the aorta encompass valves as well and these are the pulmonary and aortic valves respectively. These valves are also referred to as the semilunar valves, owing to the half-moon shape of the cusps. These valves permit blood to flow into the arteries during ventricular contraction but prevent blood from moving in the opposite direction during relaxation of the ventricle.

At the entrances at the superior and inferior venae cavae into the right atrium, and of the pulmonary veins into the left atrium no valves are normally present. However, atrial contraction pumps very little blood back into the veins as atrial contraction constricts their sides of entry into the atria, significantly increasing the resistance to backflow (Widmaier *et al.*, 2006).

1.1.2.2 Cardiac muscle

Cardiac muscle possesses properties of both skeletal and smooth muscle. The cardiac cells are notably striated as a result of the arrangement of thick myosin and thin actin filaments in such a way similar to that of skeletal muscle. Cardiac muscle cells are significantly shorter than skeletal muscle fibers and have several branching processes. Adjacent cells are joined end to end at structures known as intercalated disks, within which the desmosomes are located. The latter hold the muscle cells together and to which the myofibrils are attached. Adjacent to the intercalated disks, there are gap junctions, like those in many smooth muscles (Widmaier *et al.*, 2006).

1.1.2.3 Cardiac innervation

The heart is provided with a rich supply of both sympathetic and parasympathetic nerve fibers, the latter contained in the vagus nerve. The neurotransmitter noradrenaline (NA) is released from the sympathetic postganglionic fibers which innervate the whole heart, while the parasympathetics terminate mainly on cells found in the atria and acetylcholine (Ach) is the primary neurotransmitter released from these nerve terminals. The receptors for NA on cardiac muscle are principally β -adrenergic receptors. The hormone adrenaline, which is released from the medullary part of the adrenal gland, interacts with the same receptor as NA and exerts almost the same action in the heart. On the other hand, the receptors for Ach are of the muscarinic type (Widmaier *et al.*, 2006).

1.1.2.4 Cardiac blood supply

There is no exchange of nutrients and metabolic end products between the blood being pumped through the heart chambers and the myocardial cells. These myocardial cells, like the cells of all other organs, obtain their blood supply from arteries that branch from the aorta. The arteries providing the myocardium with blood are called the coronary arteries, and the blood flowing through these arteries is termed the coronary blood flow. From the very first part of the aorta, coronary arteries extend and lead to a branching network of small arteries, arterioles, capillaries, venules and veins similar to those in many other organs. Most of the cardiac veins drain into a single large vein called the coronary sinus, which in turn empties into the right atrium (Widmaier *et al.*, 2006).

1.1.2.5 Physiology of cardiac muscle contraction

Similar to smooth and skeletal muscle, the myocardium responds to stimulation by membrane depolarization; which leads to shortening of the contractile proteins followed by relaxation when the membrane potential returns to the resting state. Unlike skeletal muscle which demonstrates graded pattern of contraction depending on the number of muscle cells stimulated, the cells of the cardiac muscle are interconnected in groups that act in response to stimuli as a unit, contracting as one whenever a single cell is stimulated (Howland and Mycek, 2006).

1.1.2.5.a Action potential

Cardiac muscle cells are electrically excitable. However, they differ from the cells of other muscles and nerves in the fact that the cells of cardiac muscle show a spontaneous intrinsic rhythm generated by specialized “pace maker cells” located in the sinoatrial (SA), and AV nodes. The cardiac cells also encompass an uncommonly long action potential which can be divided into five distinct phases (0-4) as shown in Figure 1.3. Phase (0): represents the fast upstroke (depolarization) during which fast inward sodium (Na^+) current to the cells occurs. Phase (1): is characterized by partial repolarization as result of outward potassium (K^+) current. Phase (2): is called the plateau phase in which calcium (Ca^{2+}) is exchanged to K^+ to aid in cardiac contraction process. Phase (3): this represents the repolarization phase of the cardiac action potential during which an outward current of K^+ occurs. Phase (4): is the last phase of the action potential. It is known as forward current or spontaneous depolarization and is characterized by gradual increase in cellular permeability to Na^+ (Howland and Mycek, 2006).

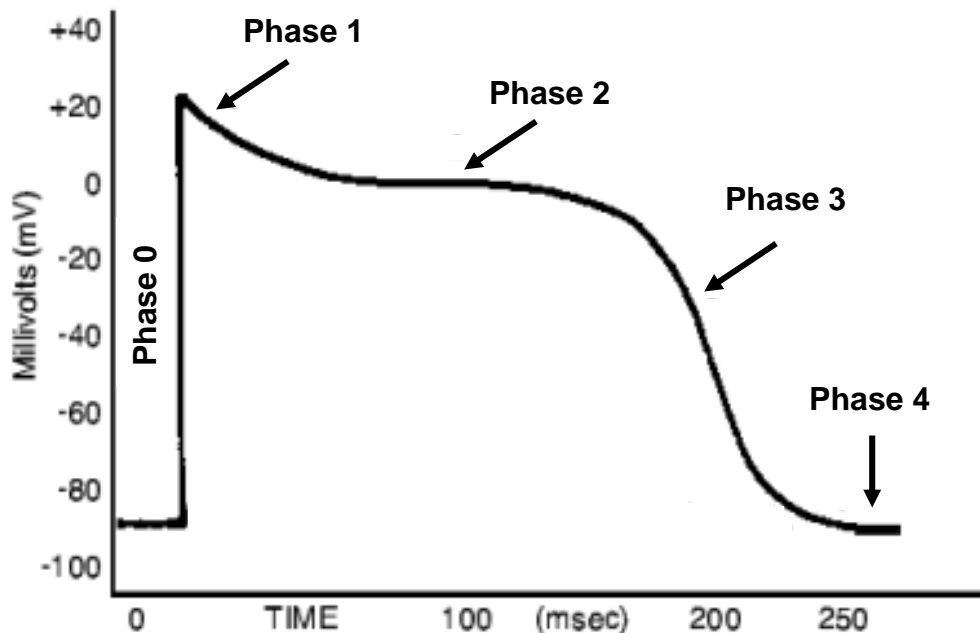


Figure 1.3: The cardiac action potential waveforms in adult human. (Adapted from Nerbonne and Kass, 2005)

1.1.2.5.b Cardiac contraction

The contractile machinery of the myocardial cell is fundamentally similar to that of striated muscle. The contraction force of the cardiac muscle is directly proportional to the concentration of free cytosolic Ca^{2+} . Hence, agents that increase Ca^{2+} levels (or increase the sensitivity of the contractile machinery) bring about an increase in the force of contraction (inotropic effect) (Howland and Mycek, 2006).

1. Sources of free intracellular calcium

Ca^{2+} principally comes from two main sources. The first source is from outside the cells, where opening of voltage-sensitive Ca^{2+} channels causes an instant rise in free cytosolic Ca^{2+} . The second source is the release of Ca^{2+} from the sarcoplasmic reticulum and mitochondria, which further increases the cytosolic level of Ca^{2+} (Howland and Mycek, 2006).

2. Removal of free cytosolic calcium

If free cytosolic Ca^{2+} level remained high, the cardiac muscle would be in a steady state of contraction. Ca^{2+} has to be removed to induce relaxation. Mechanisms of Ca^{2+} removal include:

- a. **Sodium-calcium exchange:** Ca^{2+} is removed by a sodium-calcium exchange reaction that reversibly exchanges Ca^{2+} ions for Na^+ ions across the cell membrane. This interaction between the movement of Ca^{2+} and Na^+ ions is considerable, since changes in intracellular Na^+ can affect cellular levels of Ca^{2+} .
- b. **Uptake of calcium by the sarcoplasmic reticulum and mitochondria:** Ca^{2+} is also recaptured by the sarcoplasmic reticulum and the mitochondria. Approximately more than 99% of the intracellular Ca^{2+} is situated in these organelles and even a small shift between these stores and free Ca^{2+} can lead to huge changes in the concentration of free cytosolic Ca^{2+} (Howland and Mycek, 2006).

1.1.3 Arteries and arterioles

The walls of all arteries are made up of an outer layer of connective tissue, the adventitia; a middle layer of smooth muscle, the media; and an inner layer, the intima; which is made up of the endothelium and underlying connective tissue (Ganong, 1999) (Figure 1.4). The aorta and other systemic arteries have distinctively thick walls containing large amounts of elastic tissues and therefore they provide low-resistance tubes conducting blood to the various organs and moreover act as a “pressure reservoir” for maintaining blood flow through the tissues during diastole (Widmaier *et al.*, 2006). They are stretched during systole and recoil on the blood during diastole. The walls of the arterioles have less elastic tissue but much more smooth muscle. The muscle is innervated by noradrenergic nerve fibers, which are constrictor in their function and in some cases by cholinergic fibers, which act by dilating the vessels. The arterioles are the main site of the resistance to blood flow, and little changes in their diameter result in large changes in the total peripheral resistance (TPR) (Ganong, 1999).

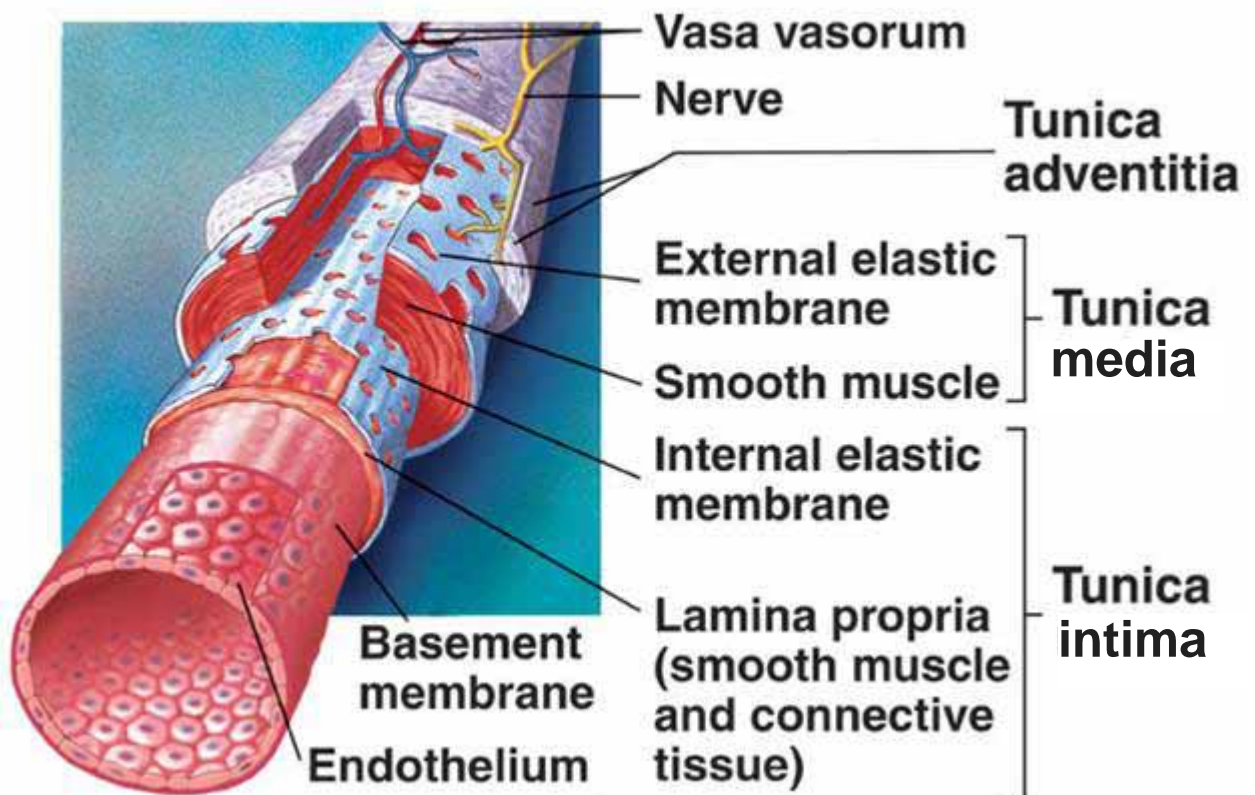


Figure 1.4: Diagrammatic section of the blood vessel. (Adapted from McKinley and O'Loughlin, 2007)

1.1.3.1 Arterial blood pressure

Ventricular contraction ejects blood into the pulmonary and systemic arteries during systole. If the amount of blood entering the artery was equal to the amount of blood flowing concurrently out of them, the total volume of blood in the arteries would remain constant and the arterial pressure would not change. However, that is not the case. The volume of blood leaving the arteries during systole is only equal to about one-third of the stroke volume and hence plays a major role in distending the arteries and elevating the arterial pressure. The overstretched arterial walls recoil reflexively and blood continues to be driven into the arterioles during diastole. As blood leaves the arteries, the arterial volume and consequently the arterial pressure fall slowly, nevertheless the subsequent ventricular contraction takes place while there is still sufficient blood in the arteries to stretch them partially. Therefore, the arterial pressure does not drop to zero.

The maximum arterial pressure reached during peak ventricular ejection is defined as systolic blood pressure (SBP), while the minimum arterial pressure occurs just before ventricular ejection commences and is termed diastolic blood pressure (DBP). In general, arterial pressure is recorded as systolic over diastolic. The difference between the values of SBP and DBP is commonly called the pulse pressure. The latter can be felt as a pulsation or throb in the arteries of the wrist or neck with each heart beat. During diastole nothing is felt over the artery, but the rapid increase in pressure at the next systole distends the artery wall and it is this expansion of the vessel that accounts for the detectable throb.

The most important factors influencing the magnitude of pulse pressure are: (1) stroke volume, (2) speed of ejection of the stroke volume, and lastly (3) arterial compliance.

Mean arterial pressure (MAP) is a meaningful measure that is sometimes used to represent blood pressure (BP). It collectively reflects both SBP and DBP. MAP is not simply the value halfway between SBP and DBP, owing to the fact that diastole lasts for a longer period than systole. The MAP is approximately equivalent to the DBP plus one-third of the pulse pressure (SBP - DBP):

$$\text{MAP} = \text{DBP} + 1/3 (\text{SBP} - \text{DBP})$$

The MAP is the most important among the pressures described since it is the pressure driving blood into the tissues averaged over the entire cardiac cycle. We can say “mean arterial pressure” without stating which artery we are referring to because the aorta and other large arteries have such large diameters that they offer only negligible resistance to flow, and the mean pressures are for that reason identical everywhere in the large arteries (Widmaier *et al.*, 2006).

1.1.3.2 Flow, pressure and resistance

Blood at all times flows from areas of high pressure to areas of low pressure. The relationship between mean flow, mean pressure, and resistance in blood vessel can be given as:

$$\text{Flow (F)} = \text{Pressure (P)} / \text{Resistance (R)}$$

Flow in any part of the vascular system is equivalent to the effective perfusion pressure in that part divided by the resistance. The effective perfusion pressure is the mean intraluminal pressure at the arterial end minus the mean pressure at the venous end. The resistance to blood flow is quantified not only by the radius of the blood vessels (vascular hindrance) but also by the viscosity of the blood.

Systemic vascular resistance (SVR) denotes the resistance to blood flow offered by all of the systemic vasculature, excluding the pulmonary vasculature. It is occasionally referred as total peripheral resistance (TPR). Those factors that influence vascular resistance in individual vascular beds are therefore the major contributing determinants of SVR. Mechanisms that result in vasoconstriction will increase SVR, while, on the other hand, those that cause vasodilatation will decrease SVR. The actual change in SVR in reaction to neurohumoral activation for example, depends upon the degree of activation and vasoconstriction, the number of vascular beds involved and the parallel arrangement of these vascular beds to each other. Even though SVR is primarily determined by changes in blood vessel diameters, changes in blood viscosity also influence SVR.

SVR can be calculated if cardiac output (CO), MAP, and central venous pressure (CVP) are known.

$$\text{SVR} = (\text{MAP} - \text{CVP}) / \text{CO}$$

Since CVP is usually near zero mmHg the calculation is often simplified to:

$$\text{SVR} = \text{MAP} / \text{CO}$$

It is very essential to note that SVR can be calculated from MAP and CO, but it is not determined by either of these variables.

A more precise way to view this relationship is that at a given CO, if the MAP is very high, it is actually because SVR is high. Mathematically, SVR is the dependent variable in the above equation; however, physiologically SVR and CO are normally the independent variables and MAP is the dependent variable (Klabunde, 2004).

1.1.4 Regulation of blood pressure

Several factors contribute to MAP regulation and these are:

1.1.4.1 Sympathetic nervous system (SNS)

Baroreceptors (pressure receptors) in both the carotids and aortic arch respond to BP changes and affect arteriolar dilation and arteriolar constriction. When baroreceptors stimulated, the contractile forces strengthen, increasing the heart rate and augmenting peripheral vascular resistance (PVR), hence increasing CO. If BP remains elevated, the baroreceptors reset at higher levels and as a result maintain the hypertension. There is little proof to suggest that adrenaline and NA have an apparent role in the etiology of hypertension. Though, many of the drugs used to treat hypertension lower BP by blocking the activity of SNS (Shargel *et al.*, 2004).

1.1.4.2 Renin-angiotensin-aldosterone system (RAAS)

Decreased renal perfusion pressure in afferent arterioles enhances renin release from juxtaglomerular cells of the kidney. The renin subsequently reacts with circulating angiotensinogen

to produce angiotensin (Ang) I (a weak vasoconstrictor). This, in turn, is hydrolyzed by angiotensin converting enzyme (ACE) to produce Ang II (a very potent natural vasoconstrictor). This vasopressor stimulates the release of aldosterone from zona glomerulosa cells of the adrenal gland, which results in augmented Na⁺ reabsorption, fluid volume and thus BP (Shargel *et al.*, 2004).

1.1.4.3 Mosaic theory

Mosaic theory centers around the fact that numerous factors, other than one factor alone, are responsible for sustaining hypertension. The interaction between the SNS, renin-angiotensin system (RAS), and potential defects in Na⁺ transport within and outside the cell may all play a contributory role in long-standing hypertension. Additional factors contributing to the development include genetics, endothelial dysfunction, and neurovascular anomalies. Other vasoactive substances that are involved in the maintenance and control of normal BP have also been recognized; these include nitric oxide (NO, vasodilating factor), endothelin (ET, vasoconstrictor peptide), bradykinin [potent vasodilator inactivated by ACE, and arterial natriuretic peptide (ANP)] (Shargel *et al.*, 2004).

1.1.4.4 Fluid volume regulation

Increased fluid volume raises venous system distension and venous return, affecting CO and tissue perfusion. These changes modify vascular resistance and increase BP (Shargel *et al.*, 2004).

1.1.5 Endothelial cells

The vascular endothelial cells serve a variety of functions:

1. Serve as a physical lining which prevents blood cells to adhere to heart and blood vessels.
2. Serve as a permeability barrier through which exchange of nutrients, metabolic end products, and fluid between plasma and interstitial fluid takes place; and by which regulation of transport of macromolecules and other substances occurs.

3. Secrete several paracrine agents that act on adjacent vascular smooth muscle cells; including vasodilators, prostacyclin (PGI₂) and NO (endothelium-derived relaxing factor, EDRF), and vasoconstrictors, notably ET-1.
4. Mediate angiogenesis (new capillary growth).
5. Play a pivotal role in vascular remodeling by detecting signals and releasing paracrine agents that act on adjacent cells in the blood vessel wall.
6. Contribute significantly to the formation and maintenance of extracellular matrix.
7. Produce growth factors in reaction to tissue damage.
8. Secrete various substances that contribute to regulation of platelet clumping, clotting, and anticlotting.
9. Synthesize active hormones from inactive precursors.
10. Extract or degrade hormones and other mediators.
11. Secrete cytokines when there are new immune responses like chemokines which is primarily secreted from damaged endothelial cells to promote the accumulation of leukocytes at the site of injury and inflammation.
12. Influence vascular smooth-muscle proliferation in the disease atherosclerosis (Widmaier *et al.*, 2006).

1.1.5.1 Endothelial vasodilating factors

1.1.5.1.a Endothelium-derived relaxation factor (EDRF)

It is a short-lived paracrine vasodilator released by the endothelial cells and is now known to be NO (Hardman *et al.*, 2006; Widmaier *et al.*, 2006). NO is the only known endogenously formed radical acting as a signaling messenger (Gewaltig and Kojda, 2002). It is formed by nitric oxide synthase (NOS), which converts L-arginine to citrulline and NO (Figure 1.5). There are three known forms of NOS (Moncada *et al.*, 1997). One form is termed constitutive, residing at the endothelial cells and releasing NO over short periods in response to receptor-mediated increases in cellular Ca²⁺ (eNOS) (Michel and Feron, 1997). The second form is responsible for the Ca²⁺-dependent release from neurons (nNOS). The third form of NOS is induced after activation of cells

by cytokines and bacterial endotoxins and, once expressed, synthesizes NO for long periods of time (iNOS). This Ca^{2+} -independent, high-output form is responsible for the inflammatory toxic manifestations of NO (Hardman *et al.*, 2006). Three analogues of L-arginine have been characterized as non selective inhibitors of eNOS: N^G -monomethyl-L-arginine (L-NMMA), N-iminoethyl-L-ornithine (L-NIO) and N^0 -nitro-L-arginine methyl ester (L-NAME) which produce concentration-dependent inhibition of the Ca^{2+} -dependent eNOS (Rees *et al.*, 1990). NO is released continuously in considerable amounts by endothelial cells in the arterioles, contributes to arteriolar vasodilation in the basal state, and has various important physiologic functions (Gewaltig and Kojda, 2002; Widmaier *et al.*, 2006). Among these functions include:

1. Regulation of BP.
2. Local vasomotion and sexual functions (penile erection and ejaculation).
3. Processing of long-term potentiation in the central nervous system (CNS).
4. Contribution to immune defense (Gewaltig and Kojda, 2002).

It has been shown that NO secretion rapidly and markedly increases in response to a large number of chemical mediators involved in both reflex and local control of arteriolar diameters. For example, NO release is stimulated by bradykinin, serotonin, purines, thrombin and histamine, substances produced locally during inflammation (Hardman *et al.*, 2006; Widmaier *et al.*, 2006). Endothelial cell-dependent mechanisms of relaxation are important in variety of vascular beds, including the coronary circulation (Hobbs *et al.*, 1999). Activation of specific G protein-linked receptors on endothelial cells promotes release of NO. Subsequently, NO diffuses readily to the underlying smooth muscle and induces relaxation of vascular smooth muscle by activating guanylyl cyclase, which increases cyclic guanosine monophosphate (cGMP) concentration. NO also has been shown to be released from certain nerves (nitrenergic) innervating blood vessels and has been found to possess a negative inotropic action on the heart (Hardman *et al.*, 2006).

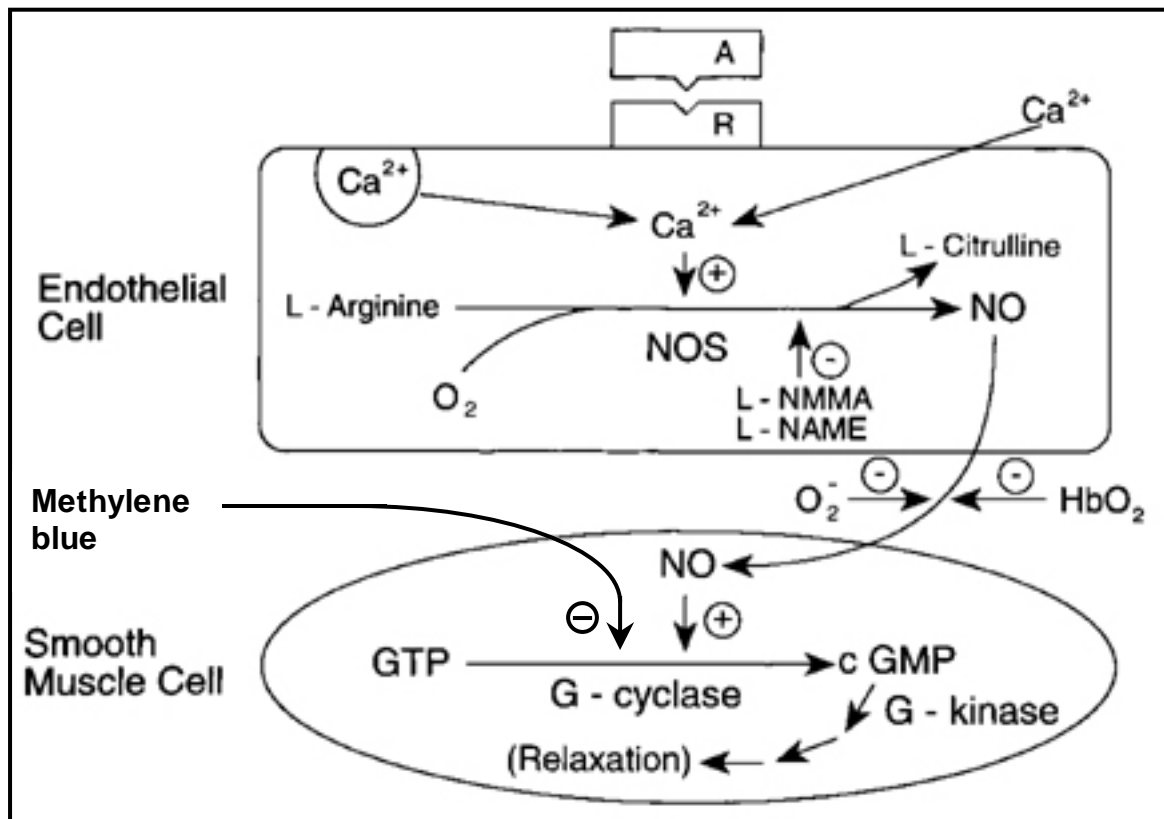


Figure 1.5: Current scheme for endothelium-dependent relaxation. Agent A, acting on receptor (R) of endothelial cell activates Ca^{2+} influx, with the increase in intracellular Ca^{2+} activating through calmodulin the eNOS, an oxygenase using L-arginine and nicotinamide adenine dinucleotide phosphate (NADPH) as co-substrates. NO diffuses to the smooth muscle cells where it activates guanylyl cyclase, with a resulting increase in cGMP, which initiates processes leading to relaxation. L-NMMA and L-NAME are arginine derivatives which inhibit NOS, and O_2^- and oxyhemoglobin (HbO_2) are potent scavengers of NO. Methylene blue acts by inhibiting soluble guanylyl cyclase. (Adapted from Furchgott, 1999)

1.1.5.1.a.i Vasodilator effects of NO

Vasodilation is the best recognized activity of NO in the cardiovascular system. This action paved the way to the discovery of EDRF almost 3 decades ago (Furchgott and Zawadzki, 1980). Subsequent research has shown that endogenous NO production plays an important role in the regulation of local vasomotion and BP (Duan *et al.*, 2003).

The mechanism underlying the NO-induced vasodilation has been extensively studied. Existing knowledge proposes an essential role for cGMP-dependent activation of protein kinase

(PKG I) which possesses the ability to phosphorylate various membrane proteins in the sarcoplasmic reticulum (Figure 1.6). The latter pathway of cGMP is antagonized by the action of the soluble guanylate cyclase inhibitor methylene blue [phenothiazin-5-ium,3,7-bis(dimethylamino)-, chloride, trihydrate], (Figure 1.5) (Duan *et al.*, 2003).

It has been stated that PKG I is capable of phosphorylating phospholamban (Cornwell *et al.*, 1991). In its dephosphorylated form, phospholamban monomers inhibit the sarcoplasmic reticulum ATPase (SERCA) by interacting with its cytoplasmic and membrane domains resulting in Ca^{2+} pump aggregation. Phosphorylation of phospholamban (example by PKG I) causes the union of phospholamban monomers into pentamers and reverses the inhibition of SERCA (Simmerman and Jones, 1998). This triggers a fast sequestration of intracellular Ca^{2+} , which in turn also decreases the influx of extracellular Ca^{2+} into the sarcoplasmic reticulum (Cohen *et al.*, 1999).

Another latest report reveals that activation of PKG I phosphorylates a newly-discovered protein, the 1,4,5-inositoltriphosphate (IP_3) receptor associated cGMP kinase substrate (IRAG) (Schlossmann *et al.*, 2000). A strong inhibition of IP_3 -evoked Ca^{2+} release from the sarcoplasmic reticulum is produced by phosphorylation of IRAG. Recently, it is still unknown how IRAG phosphorylated by PKG I binds to IP_3 receptor. NO has also the ability to activate Ca^{2+} -dependent K^+ channels and therefore augments the outward K^+ current (Bolotina *et al.*, 1994). The consequential hyperpolarization of the cell membrane reduces the effect of the depolarizing signals and induces vasodilation (Figure 1.6). Reports have shown that this effect of NO can be both independent and dependent on activation of PKG I (Bolotina *et al.*, 1994; Sausbier *et al.*, 2000). Finally, the mechanism of vasodilation induced by NO might also involve the cGMP-dependent inhibition of voltage-gated Ca^{2+} channels (Ishikawa *et al.*, 1993). Remains to be determined, is the relative contribution of each of these PKG I- and K^+ channel-dependent vasodilating mechanisms of NO. The subsequent decline of the intracellular Ca^{2+} concentration reduces the formation of the Ca^{2+} -calmodulin-myosin light chain (MLC) kinase complex. This decreases phosphorylation of

Ser19 in the myosin regulatory light chains and ultimately inhibits vasoconstriction (Horowitz *et al.*, 1996).

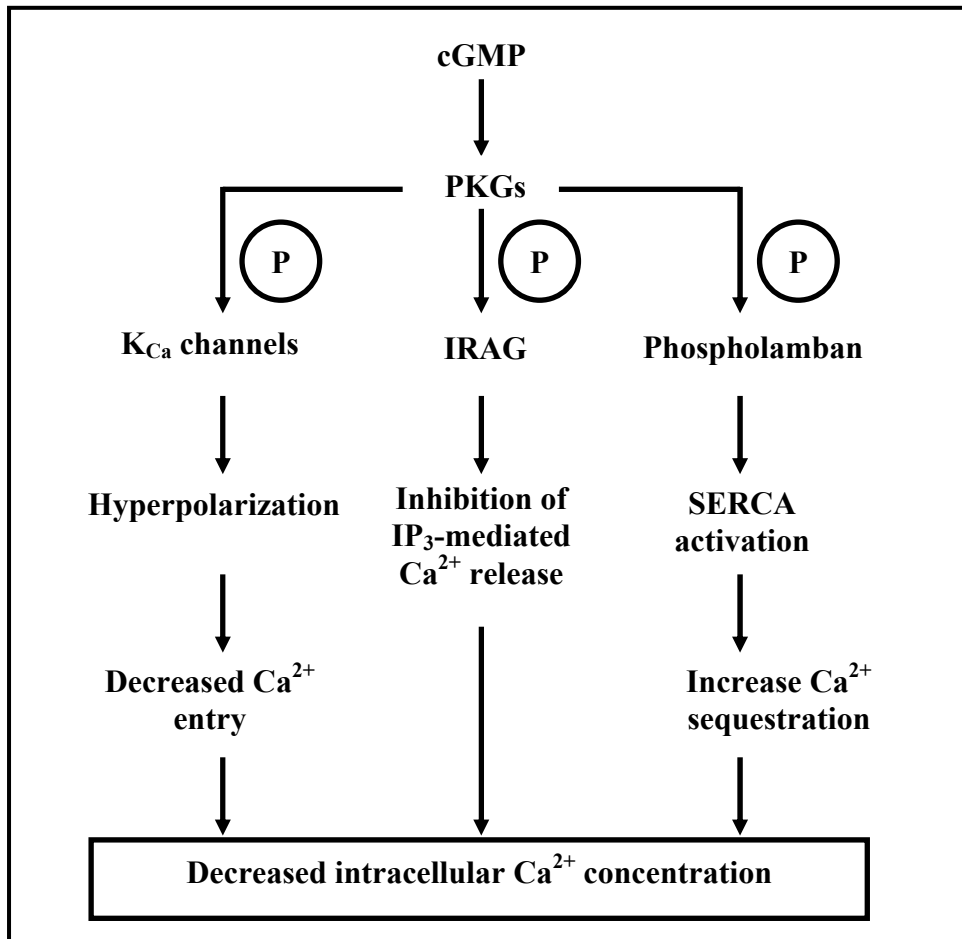


Figure 1.6: Mechanisms of vasorelaxation induced by NO. After the activation of soluble guanylyl cyclase, cGMP is formed which in turn stimulates cGMP-dependent protein kinases (PKGs). Subsequently, three important proteins are phosphorylated resulting in a decrease of the intracellular Ca^{2+} concentration. The direct effect of NO on K^+ channels and the cGMP-dependent inhibition of voltage-gated Ca^{2+} channels is not shown; K_{Ca} channels = Ca^{2+} dependent K^+ channels; IP_3 = 1,4,5-inositol trisphosphate; IRAG = IP_3 receptor associated cGMP kinase substrate; SERCA = sarcoendoplasmic reticulum ATPase. (Adapted from Gewaltig and Kojda, 2002)

1.1.5.1.a.ii Modulation of sympathetic activity

NO acts as a neuromodulator not only within the CNS but also within peripheral autonomic pathways controlling cardiac function to provide a net enhancement of parasympathetic and inhibition of sympathetic control (Chowdhary and Townend, 1999). Up to 40% of intrinsic cardiac neurons contain nNOS (Armour *et al.*, 1995), including those innervating the nodal regions

(Klimaschewski *et al.*, 1992). eNOS has been identified within SA node, myocytes, and their adjacent capillaries (Han *et al.*, 1998). The NO generated at these peripheral cardiac autonomic sites appears to enhance not only the heart rate response to vagus parasympathetic nerve stimulation (Elvan *et al.*, 1997; Conlon and Kidd, 1999; Choate *et al.*, 2001; Herring and Paterson, 2001) but also parasympathetic antagonism of cardiac sympathetic responses, which is an indirect activity (Elvan *et al.*, 1997; Sears *et al.*, 1998). Endogenous NO acts at a postsynaptic level to facilitate cardiac responses to muscarinic stimulation when background levels of adrenergic activity are high.

Furthermore, NO has also been shown to directly inhibit cardiac responses to sympathetic stimulation in animals (Balligand, 1999) by presynaptic rather than postsynaptic mechanisms. This presynaptic action of NO has recently been confirmed by evidence that both NO donors and more specifically adenoviral nNOS gene transfer to the guinea pig right atrium increases Ach release from vagal nerve terminals in response to electrical stimulation (Herring and Paterson, 2001; La Rovere *et al.*, 2001).

NO has been shown to cause a cGMP-dependent inhibition of the adrenergically isoprenaline (ISP)-stimulated inward Ca^{2+} current, a mechanism believed to mediate, at least in part, the indirect muscarinic response. No effect of NO on the stimulation of the Ach-gated outward K^+ current (direct muscarinic pathway) was evident (Han *et al.*, 1998).

1.1.5.1.a.iii Antiplatelet effects of NO

Platelets play a central role in vascular hemostasis. Their ability to aggregate and produce a hemostatic plug must be carefully balanced against the need to maintain the fluid state of the blood and to avoid thrombosis (Radomski and Moncada, 1993). Platelet hyperactivity is one of the leading causes of atherosclerotic changes associated with thrombosis, myocardial infarction (MI) and stroke. NO and NO donors excite cGMP production in human platelets resulting in activation of PKG and inhibition of platelet aggregation induced by agonists (for example thrombin which

increase the intracellular Ca^{2+} concentration) (Benjamin *et al.*, 1991; Moro *et al.*, 1996). It is clear how NO-induced inhibition of platelet aggregation results in reduction in the intraplatelet Ca^{2+} concentration (Rao *et al.*, 1990). Comparable to the mechanism of NO-induced vasorelaxation, NO-induced inhibition of platelet aggregation involves phospholamban- and SERCA-dependent refilling of intracellular Ca^{2+} stores (Nguyen *et al.*, 1991; Trepakova *et al.*, 1999). Additionally, cGMP has been shown to indirectly activate cyclic adenosine monophosphate (cAMP) protein kinase PKA, since cGMP inhibits the breakdown of cAMP by phosphodiesterase, PDE III (Bowen and Haslam, 1991). Both nucleotides are known to possess the ability to phosphorylate phospholamban, which then activates SERCA to promote the sequestration of Ca^{2+} (Fischer and White, 1987; Geiger *et al.*, 1994). NO and cGMP analogues perform their actions synergistically with cAMP-elevating agents such as PGI_2 to inhibit platelet aggregation (Bowen and Haslam, 1991). To sum up, both cAMP and cGMP-elevating agents inhibit platelet aggregation by a reduction of the intracellular Ca^{2+} concentration.

1.1.5.1.a.iv Antiadhesive effects of NO

NO is an essential endogenous mediator which inhibits leukocyte adhesion (Kubes *et al.*, 1991). NO released by NO donors has been discovered to potently inhibit the expression of vascular cell adhesion molecule (VCAM-1) (Khan *et al.*, 1996), while an opposite effect is seen when endogenous NO synthesis is inhibited (Niu *et al.*, 1994). Khan *et al.* (1996) presented that this action of NO is mediated by inhibition of nuclear factor κB (NF κB), a redox sensitive transcription factor, expression and involves the antioxidative properties of NO. Oxidation of polyunsaturated fatty acids such as linoleic acid to peroxidized metabolites seems to be a central intermediate step in cytokine-induced activation of NF κB and this oxidation can be significantly reduced by exogenous NO. Similarly, increased leukocyte adhesion induced by the inhibition of NO synthases is at least partially reversed by various intracellular oxygen radical scavengers (Niu *et al.*, 1994). Therefore, the mechanism of the antiadhesive action of NO most probably involves antioxidative effects.

1.1.5.1.a.v Antiproliferative effects of NO

NO has been reported to inhibit smooth muscle proliferation. This applies for both NO generated by the vascular endothelium (Scott-Burden and Vanhoutte, 1993) and NO produced by NO donors (Nakaki *et al.*, 1990).

The mechanism underlying the antiproliferative activity of NO is yet to be fully explained. It has been suggested that cGMP-dependent activation of PKA, partially mediated by the inhibition of the cGMP-inhibited-cAMP PDE III may play a role (Cornwell *et al.*, 1994; Osinski *et al.*, 2001). Another key mechanism underlying the antiproliferative effects of NO, which takes place independent of cGMP generation, is the inhibition of arginase ornithine decarboxylase (Ignarro *et al.*, 2001). Experiments on rat aortic smooth muscle cells have confirmed that antiproliferative concentrations of NO donors strongly diminish the cellular content of polyamines such as putrescine, spermidine, and spermine and inhibit the activity of purified ornithine decarboxylase (Gewaltig and Kojda, 2002).

1.1.5.1.a.vi Antioxidant effects of NO

Vascular oxidative stress has been shown to contribute to the pathophysiology of cardiovascular diseases. Among the various reactive oxygen species (ROS) formed under these circumstances, superoxide is apparently the main one (Kojda and Harrison, 1999). The complex interactions of oxygen species with vascular signaling systems have been recently reviewed (Wolin, 2000). The best known antioxidative effect of NO is the impairment of lipid oxidation. NO can potently inhibit the oxidation of free fatty acids, phosphatidylcholine and low density lipoprotein particles. In view of the proatherogenic effects of oxidized lipids, this antioxidative activity of NO is likely to be relevant (O'Donnell and Freeman, 2001).

NO reacts very rapidly with superoxide to form peroxynitrite (ONOO^-) which is a much stronger oxidant than superoxide itself. *In vivo*, ONOO^- rapidly forms a carbonate adduct (ONOOCO_2^-) or oxidizes free undissociated thiols (Koppenol, 1998). The carbonate adduct can

rapidly form carbonate and nitrogen dioxide radicals (Bonini *et al.*, 1999). Recently, these radicals have been shown to oxidize thiols to thiyl, sulfinyl and disulfide radicals (Bonini and Augusto, 2001). The oxidizing potential of ONOO⁻ and the subsequently formed radicals facilitate lipid peroxidation, induce protein damage by tyrosine nitration, dityrosine formation and thiol oxidation and reduce the antioxidative capacity of vascular cells by the rapid oxidation of free undissociated thiols (Radi *et al.*, 1991; Pfeiffer *et al.*, 2000; Bonini and Augusto, 2001).

In view of these reactions, it seems rather doubtful that the increased generation of NO in the setting of oxidative stress might be associated with antioxidative properties or might augment the antioxidative power of vascular wall. Nevertheless, the formation of ONOO⁻ from superoxide competes with hydrogen peroxide (H₂O₂) formation catalyzed by superoxide dismutases (SODs), (Figure 1.7).

Even though superoxide reacts just about 3–6 times faster with NO than with SOD, the formation of ONOO⁻ is outcompeted if the concentration of SOD is much greater than that of NO, a situation that is frequently found in the intracellular space of vascular endothelial and smooth muscle cells (Koppenol, 1998). Accordingly, physiologic concentrations of vascular NO, as generated by eNOS or by therapeutic interventions, possibly exert antioxidative effects in the presence of physiologic concentrations of SODs (Beckman and Koppenol, 1996). On the contrary, very high concentrations of NO, as generated by iNOS, apparently promote ONOO⁻ formation.

Another antioxidative effect of NO is by means of the induction of extracellular SOD (ecSOD) which has been shown to rise *in vitro* and *in vivo* (Fukai *et al.*, 2000). This powerful antioxidative enzyme is expressed in vascular smooth muscle cells and situated at the outer cell membrane. In the vascular wall 1/3–1/2 of the total SOD is the extracellular type of the enzyme (Stralin *et al.*, 1995). The up-regulation of ecSOD expression in vascular smooth muscle cells may signify an essential mechanism that averts superoxide-mediated degradation of endothelial NO as it traverses between the two cell types. Similarly, the formation of ONOO⁻ will be less, because higher

amounts of SOD favors the dismutation of superoxide to H_2O_2 (Koppenol, 1998). Lately, it was stated that just a brief exposure of endothelial cells to the strong oxidant H_2O_2 can enhance the expression and activity of eNOS (Drummond *et al.*, 2000), a mechanism that might account for the antioxidative effects of NO.

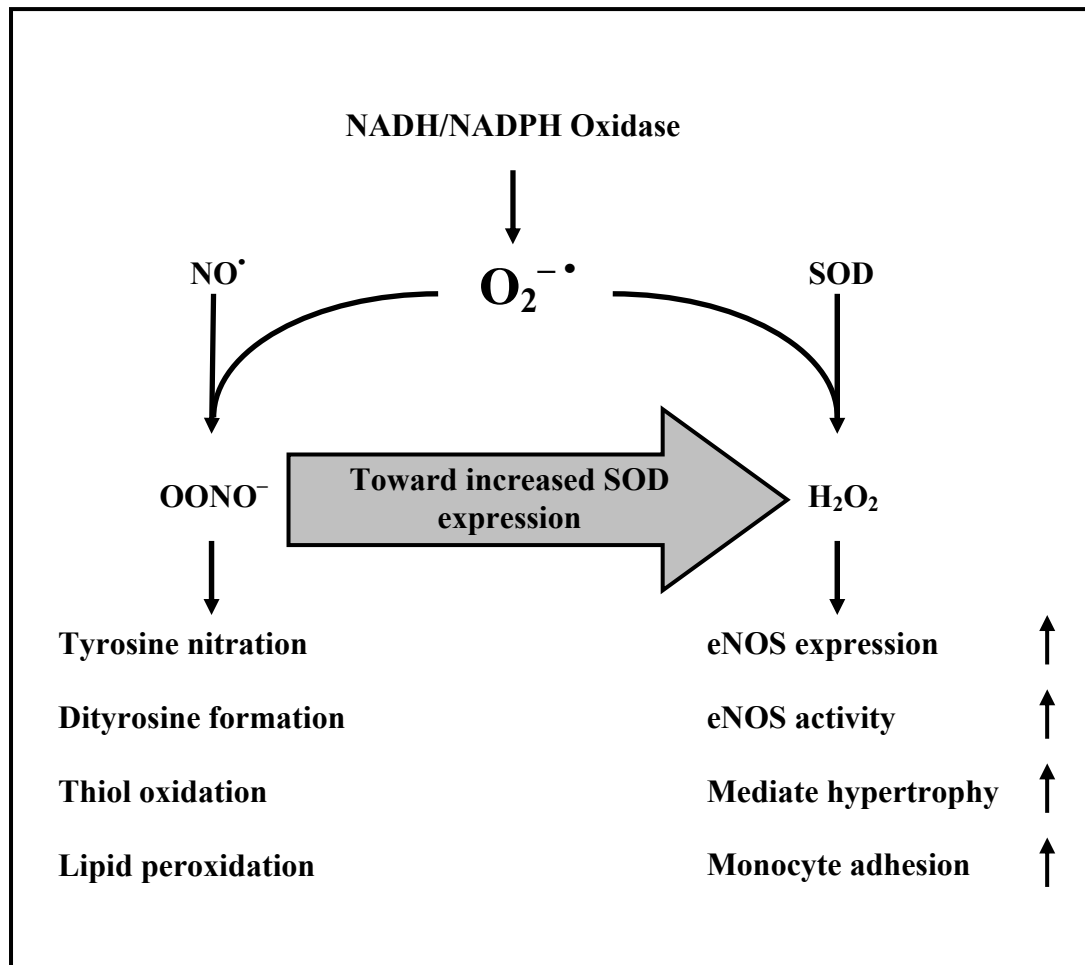


Figure 1.7: Reactions of $\text{O}_2^{-\bullet}$ with SOD and NO. The reaction constants and the mean concentrations of intracellular and membrane-associated SOD and of NO in the vascular wall suggest that the formation of H_2O_2 is favored. In addition, an increase of SOD expression as induced by exercise and NO would further shift the balance to H_2O_2 formation. The role of H_2O_2 as a vascular oxidant is unclear. Both, vasoprotective actions and proatherosclerotic actions have been reported. NO^\bullet = nitric oxide radical, $\text{O}_2^{-\bullet}$ = superoxide anion, SOD = superoxide dismutase, OONO^- = peroxynitrite, H_2O_2 = hydrogen peroxide, NADH = nicotinamide adenine dinucleotide, NADPH = nicotinamide adenine dinucleotide phosphate and eNOS = endothelial nitric oxide synthase. (Adapted from Gewaltig and Kojda, 2002)

1.1.5.1.b Prostacyclins (PGI₂)

PGI₂ is considered the main eicosanoid synthesized by endothelial cells (Moncada, 1977). The biosynthesis of PGI₂ by endothelial cells is initiated either via a transmembrane transfer of prostaglandin endoperoxides from platelets (Bunting *et al.*, 1976; Shafer *et al.*, 1984) or by intracellular production from arachidonic acid (AA), which is released from endothelial phospholipids by an activated phospholipase (Hong and Deykin, 1982; Lambert *et al.*, 1986). PGI₂ has a broad range of effects as it acquires antiplatelet, antiadhesive, vasodilatory and antiproliferative properties (Vane, 1978; FitzGerald and Patrono, 2001). The main biological actions of PGI₂ are mediated by the PGI₂ receptor (IP), which is a G-protein coupled receptor. PGI₂ appears to play an important protective role against elevated BP, as it has been shown that deletion of the IP promotes salt sensitive hypertension and cardiac fibrosis in mice (Francois, 2005). Several studies show that prostaglandins and PGI₂ especially, excite baroreceptor neurons (BRNs), as well as cardiac vagal afferents (Xie *et al.*, 1990; Brandle *et al.*, 1994; Ustinova and Schultz, 1994; Schultz, 2001). Diminished synthesis of PGI₂ may take part in acute and chronic baroreceptor resetting and the reduced baroreceptor sensitivity in hypertension (Xie *et al.*, 1990; Wang *et al.*, 1993). PGI₂ liberated by ischemic myocardium activates cardiac vagal afferents and depresses the baroreflex (Zucker *et al.*, 1989).

For so many years, endothelial cell generation of PGI₂ was thought to be mediated by cyclooxygenase (COX) enzyme, COX-1, based on *in vitro* studies (Mitchell and Warner, 2006). Yet, studies have demonstrated that COX-2 is the foremost contributor to systemic PGI₂ as assessed by urinary excretion of PGI₂ metabolites, but the relative contributions of COX-1 and COX-2 [the action of both is inhibited by indomethacin (Ajay *et al.*, 2007)], to endothelial PGI₂ production *in vivo* stay a subject of debate, with most evidence pointing to COX-1 as the main enzyme isoform involved (Flavahan, 2007).

The platelet-suppressant and vasodilator effects of PGI₂ (Moncada and Vane, 1979; Gryglewski, 1980; Whittle and Moncada, 1984) are principally interceded by the stimulation of